Florida International University

FIU Digital Commons

7-2-2021

Low-cost and Reliable Integrated Hardware and Software Framework for Remotely Operated Water Release from Storage Units

Vivek Verma
Florida International University, vverm002@fiu.edu

Follow this and additional works at: https://digitalcommons.fiu.edu/etd

Part of the Civil Engineering Commons, and the Environmental Engineering Commons

FLORIDA INTERNATIONAL UNIVERSITY

Miami, Florida

LOW-COST AND RELIABLE INTEGRATED HARDWARE AND SOFTWARE

FRAMEWORK FOR REMOTELY OPERATED WATER RELEASE FROM

STORAGE UNITS

A dissertation submitted in partial fulfillment of

the requirements for the degree of

DOCTOR OF PHILOSOPHY

in

CIVIL ENGINEERING

by

Vivek Verma

2021

To: Dean John L.Volakis
    College of Engineering and Computing

This dissertation, written by Vivek Verma and entitled, Low-cost and Reliable Integrated Hardware and Software Framework for Remotely Operated Water Release from Storage Units, has been approved regarding style and intellectual content, is referred to you for judgment.

We have read this dissertation and recommend that it be approved.

_____

Hector R. Fuentes

_____

Paul Indeglia

_____

Seung Jae Lee

_____

Ou Bai

_____

Arturo S. Leon, Major Professor

Date of Defense: July 02, 2021

The dissertation of Vivek Verma is approved.

_____

Dean John L. Volakis
College of Engineering and Computing

_____

Andr'es G. Gil
Vice President for Research and Economic Development
and Dean of the University Graduate School

Florida International University, 2021

DEDICATION

This study is wholeheartedly dedicated to my beloved parents, who have been my source

of inspiration and gave me strength when I thought of giving up, who continually provide

their moral, spiritual, emotional, and financial support.

To my brothers, sisters, relatives, mentors, friends, and classmates who shared their

words of advice and encouragement to finish this study.

And lastly, I dedicated my dissertation to the Almighty God; thank you for the guidance,

strength, power of mind, skills, protection, and for giving us a healthy life.

All of these, I offer to you.

ACKNOWLEDGMENTS

ABSTRACT OF THE DISSERTATION

LOW-COST AND RELIABLE INTEGRATED HARDWARE AND SOFTWARE

FRAMEWORK FOR REMOTELY OPERATED WATER RELEASE FROM

STORAGE UNITS

by

Vivek Verma

Florida International University, 2021

Miami, Florida

Professor Arturo S. Leon, Major Professor

The main contribution of this research is towards the broader area of water management that can be used for multiple purposes. For instance, floods can be mitigated using a novel approach based on the integrated dynamic management of water storage units such as reservoirs, wetlands, and ponds. This approach will enable adaptive water release from storage units hours or days ahead of rainfall events, thereby maximizing storage capacity and minimizing flooding.

This approach can be implemented by retrofitting water storage units using siphon hydraulic systems and are remotely controlled in an integrated manner using the decision support system. To make it feasible in a relatively inexpensive way, this dissertation developed a modular, scalable, and integrated hardware-software platform for interfacing automated siphons/gates, sensors, and sensor control/communication to enable remote operation of hundreds and thousands of

gates in storage units. In this study, a siphon hydraulic system was developed and used to implement and test the hardware and software integrated control system.

The hardware architecture includes water level sensors, bilge pump, air-vent, and actuated butterfly valve. The software architecture is designed and developed in C-sharp language and displays near real-time data from the sensors employed in the lab. It also displays the functioning or malfunctioning condition of all digital and analogic lab hardware. The latter can be used to schedule maintenance operations without visiting the lab.

Various cutting-edge technologies such as the Internet of Things (IoT), Software Defined Radios (SDR), and Virtual Private Network (VPN) is employed to integrate the hardware and software architecture. All the data collection and operations are performed remotely using 4G/5G cellular communication. Extensive experiments were performed in the lab, and the results indicate that the systems are reliable. Reliability is defined as the probability that the system will perform its intended function adequately without failure.

The operational reliability of sensors and other field hardware, such as liquid level sensors, bilge pumps, and air vents, has been analyzed using the Reliability Block Diagram (RBD) using the ExtendSim software. In this method, the components of the system are linked through graphic blocks following their functional logic or operational relationship. The results of the operational reliability of the system are obtained through Monte Carlo simulations.

TABLE OF CONTENTS

LIST OF TABLES

LIST OF FIGURES

CHAPTER 1: INTRODUCTION

1.1 Introduction and literature review

Billions of dollars in infrastructure and property damages and hundreds of human lives are lost each year because of natural disasters such as hurricanes and storms (Demir and Kisi, 2016). The global average annual economic losses caused by floods in the 20th century amounted to US$ 30 billion, accounting for about one-third of the total economic damage caused by various natural disasters. The death toll from floods in the 20th century was below that of plagues and droughts (Shao et al., 2018). Nevertheless, about 2.8 billion people were affected by floods from 1980 to 2009, leaving 4.5 million left people homeless, about 540,000 deaths, and 360,000 injuries (Subyani et al., 2017). Adverse water quality alteration effectively results in large-scale illness and deaths, accounting for around 50 million deaths worldwide per year, mainly in Africa and Asia (Praveen et al., 2016).

Flood is generally caused by heavy rains, leading to overflowing rivers and exacerbated through inadequately designed urban drainage systems, encroachment into flood plains, and structural failure of infrastructure. The solution of flood problems in the basin can be addressed by strategically installing wetlands on hydraulic soils in the nearest areas (Leon and Verma, 2019) and by building an integrated plan to control flooding, including the use of wetlands to intercept and retain precipitation and to store floodwaters in those areas (Hey and Philippi, 1995; Verma et al., 2020b). In addition, the introduction of a control structure such as sluice gates may play a key role in balancing a load of discharges through

various river system branches, thereby decreasing the risk of flooding in susceptible hydraulic basins (Chou and Wu, 2015; Mel et al., 2020).

Various strategies have been adopted to cope with flood hazards, which can be categorized into two contrasting types, structural and nonstructural (Thampapillai and Musgrave, 1985). Structural measures are strategies to reduce floods using various rigid structures, such as levees, floodwalls, dams, seawalls, and other appurtenant structures (Son et al., 2015). Nonstructural measures include flood warning and evaluation and floodplain land-use (Breckpot et al., 2010). This study presents a structural measure that can be effective for flood management by using integrated management of water storage units such as reservoirs, wetlands, and ponds (Leon et al., 2018; Verma et al., 2020a).

Control gates are used to mitigate floods from very small to the Probable Maximum Flood (PMF), without forecasting the flood hydrograph's actual scale (Yigzaw et al., 2013). Such gates' operation is complex since the actual severity of an incoming flood can only be anticipated in advance for most streams unless a sophisticated network of precipitation and flow gauges exists in the catchment (El Afandi et al., 2013). Failure of gate operation arises because identifying the most effective operation of the drainage gates is a complex issue, and it depends on the intensity of flood hydrograph, availability of flood retention storage volume, the flow rate of downstream (Sene, 2008).

Due to enhanced flood frequency and intensity (Kang et al., 2019; Kunkel, 2003), new emphasis is placed on assessing the effectiveness of flood mitigation methods (Qin et al., 2019). Within a watershed, storage units play an important role in minimizing flooding by

storing water (Lee et al., 2009; Ming et al., 2007; Mitsch et al., 2015). Several studies have demonstrated the efficacy of storage systems (Bekele and Nicklow, 2007; Bullock and Acreman, 2003; Green et al., 2000) for flood mitigation. However, in many cases, their effectiveness appears to be limited by the limited storage capacity.

This study proposes a structural way that can be used to mitigate flooding using gate operations and siphon systems optimal utilizing storage units such as wetlands, ponds, and reservoirs. Gate operation is one of the vital aspects with the help of which flood can be alleviated. Gate operation can be performed once other information such as when, how frequently, how long gate operation should be performed, etc. This information can be obtained using various modeling processes such as weather forecasting and hydrological modeling (Abdelkarim et al., 2019; Knebl et al., 2005).

Supervisory Control and Data Acquisition (SCADA) is a control system used to acquire data, has a manual/automatic control option, and monitors the entire process (Daneels and Salter, 1999; Foh and Lee, 2004). The working of SCADA system consists of three key components: collection, transmission, and control mechanism; all work collectively to run the whole system (Goel and Mishra, 2009). The proposed siphon hydraulic system is analogous to the SCADA system as it employs similar key components (Ozecik, 2021). SCADA system is one of the most popular systems that is used in almost every industry such as sea industry, oil and gas processing, water quality, power, and water storage (Gao et al., 2010)

1.2 Project overview

The present work in this dissertation is a part of a big and more comprehensive project, as shown in Fig. 1.
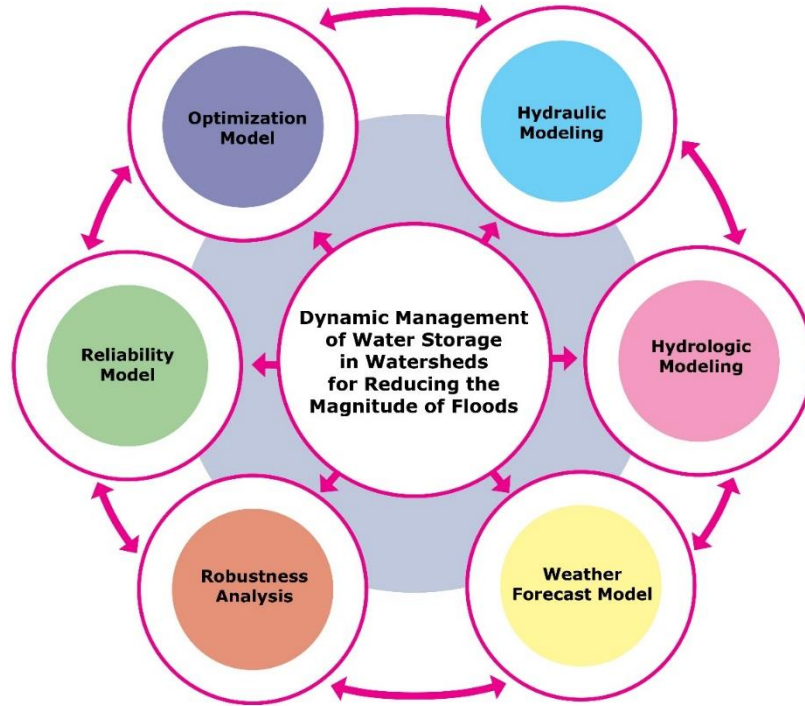
Figure 1. Project Overview

The project consists of several models: the weather forecast model, hydraulic and hydrologic model, optimization and reliability model, and robustness analysis for the entire framework. All of these models will be a part of a single platform. The weather forecast model will predict a storm event that may result in flooding hours or days ahead of rainfall events. The hydrologic model will estimate the amount of runoff that will be generated from the forecasted event. The optimization model will determine the optimum amount of water released from storage units to prevent/reduce flooding. Gate operations will be performed remotely to release water. The hydraulic model will analyze streamflow

characteristics such as depth, width, flow velocity, etc. Finally, reliability and robustness analysis will be performed for the entire framework to ensure consistency and ensure that the system continues to function under different environmental conditions.

1.3 Research objectives

This research aims to develop a low-cost, reliable, and integrated hardware-software platform for the operation of storage units (reservoirs, wetlands, and ponds) that can be used for multiple purposes. The hardware architecture is developed to collect, transfer, and operate field data to a remote computer. A software interface is also designed to monitor and control gate operations of siphon hydraulic systems to release water from storage units remotely. The interface will also be used to check the functioning or malfunctioning of the field devices and schedule maintenance activities. This research also evaluates the operational reliability of various components such as liquid level sensors, bilge pumps, and air vents using the Reliability Block Diagram (RBD) in the ExtendSim software. This research also estimates the cost analysis of the proposed systems for nine scenarios that consist of three redundancies and three periods of maintenance for three life spans.

CHAPTER 2: ARCHITECTURE FOR REMOTE CONTROL OF WATER RELEASE IN A NETWORK OF STORAGE UNITS USING A RADIO COMMUNICATION SYSTEM

2.1 Overview of the proposed system

2.1.1 Hardware architecture

The overall hardware architecture is presented in Fig. 2. As shown in Fig. 2, the architecture consists of water level sensors, PLC, master and slave SDR, and cellular router. SDR is a radio communication system where components that have been typically implemented in hardware are instead implemented using software on a personal computer or embedded system. All the data from sensors are collected by the slave SDRs, which transmit it to the master SDR. The master SDR then transfers the data to the control hub using a router that uses a 3G/4G cellular connection. A sub-system consists of sensors, PLCs, and slave SDRs. A PLC collects input from the sensors and controls the pump and actuator accordingly. Each PLC is connected to an SDR as a low-cost method for serving as a link between the slaves and the master SDR; multiple sub-systems can be employed in the lab connected to a master SDR.

The SDRs will transmit their signals through custom-designed, low-cost, in-house fabricated circular monopoles. The master system can be accessed by remote connection via cellular router connection. Since all the sub-systems are connected to the master system, connections to all the sub-systems can be made through the same router.
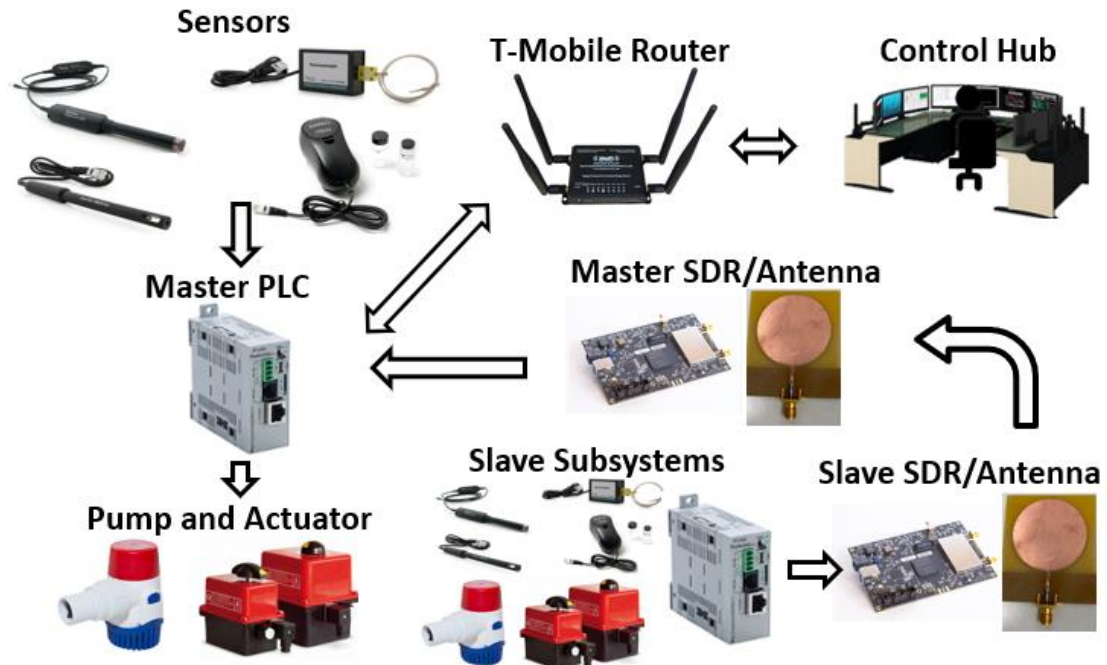
Figure 2. Overview of components of the proposed architecture

2.1.2 Radio engineering design of antenna and SDR for control hub link

The wireless part of the system was implemented with an SDR and a custom-made antenna. The SDR was a BladeRFx40 which is easily programmable to transmit and receive text files. The program was coded with open source GNURadio and Python 2.7 to achieve a narrowband frequency modulated (NBFM) signal. Since the data packets being sent are relatively small, it was simple to ensure the industry standard of 10^{-3} bit error rate (BER) by simply providing ample signal-to-noise ratio (SNR) and repetitive transmissions. Typical Gaussian noise was assumed with a Rayleigh fading channel to ensure robustness against multipath effects. Thus, line-of-sight (LOS) and multiple alternate paths were assumed to reach the receiver. In addition, the repetitive transmissions were tuned at a time interval greater than the longest multipath signal to prevent signal collisions. For proof-of-

concept, the system was tested in a lab-controlled environment with two BladeRFx40, and successful transmission of the text files was observed.

A circular monopole antenna was constructed to transmit and receive these signals. The antenna's omnidirectional nature makes it an ideal candidate for sending and receiving signals from multiple directions, thus minimizing the need for on-site tuning. Nevertheless, the Omni-direction pattern usually suffers from lower gain. To compensate for this, the antenna was designed to operate at a lower frequency (viz. 700MHz), where a more extended range can be achieved. This is verified using Frii's equation in free space. A comparison of a range of signals transmitted with the same power at 700MHz and 2.4GHz monopole is shown in Fig. 3. Clearly, the received power at 700MHz is 10-fold higher than the received power at 2.4GHz.
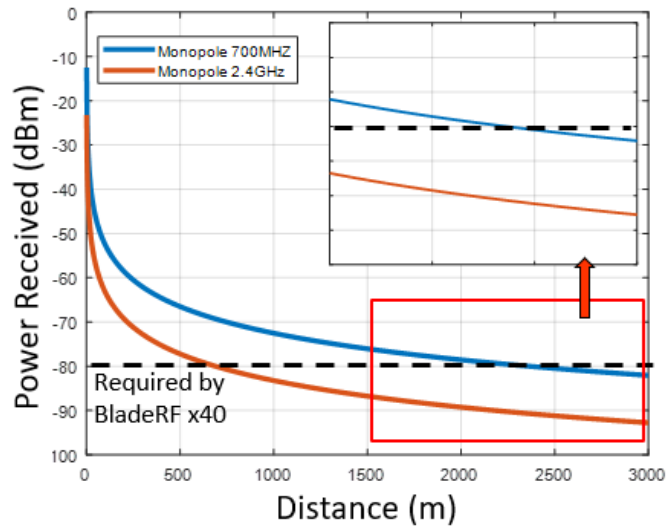
Figure 3. Link budget analysis for monopole antennas at 700MHz and 2.4GHz with a minimum required received power from the BladeRF x40 marked with dashed lines

These types of studies are commonly referred to as link budget analysis. Here the same transmitting power and the transmitting and receiving gain of 2.4dB in both antennas were assumed. The lower frequencies can meet the BladeRF x40 minimum receive power limits at a much further range of about 2.5km. As such, a circular monopole was designed and fabricated in-house on low-cost FR4 material. The antenna was designed to have a reflection coefficient of less than -10dB. This ensures that at least 90% of the power inserted into the antenna is radiated out. In Fig. 4, the measured gain of the antenna shows 2.4dB at 700MHz.
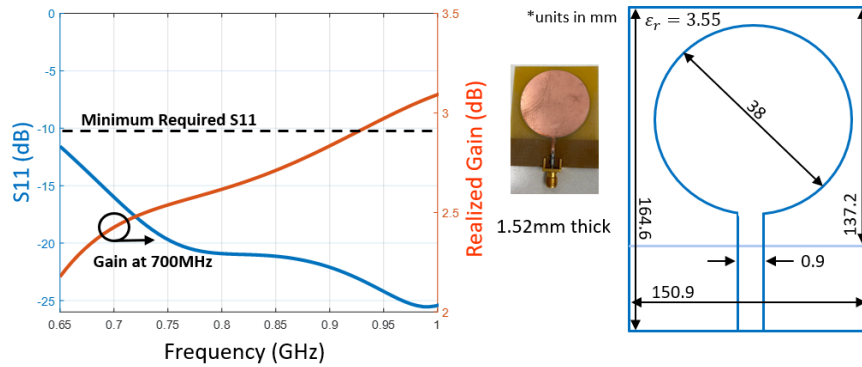
Figure 4. Measured Monopole antenna S11 and realized gain from 650-1000 MHz and antenna dimensions

2.1.3 Control system interface between radio, sensors, pump, and actuator

The master and slave PLCs serve different functions to satisfy the system requirements. Therefore, two distinct algorithms are required. First, the slave PLC must read data from level sensors, control pump, and the actuator. And then, each slave PLC must be able to transmit this information to the master PLC through an SDR. After that, the master PLC will relay the slave information to the control hub via the cellular router connection. The two algorithms for the master and the slave SDRs are shown in Table 1.

Table 1. Algorithm for master and slave SDR

Algorithm for master PLC

while (1)

      read (data from level sensors)

      write (pump/actuator response)

      read (slave data from BladeRF)

      write (master and slave data to router)

end

Algorithm for slave PLC

while (1)

      read (data from level sensors)

      write (pump/actuator response)

      write (sensor data and response to BladeRF)

end

2.2 Integrated control software

The integrated control software was written in C#, a widely-used programming language, to remotely control single or multiple storage units' hardware. Fig. 5 illustrates the main software interface. Fig. 6 present the software interface for an actuated gate's remote operation in a siphon (S1). As shown in Fig. 6, a siphon requires four water level sensors, one air vent, one actuated valve (e.g., butterfly valve), and one pump (e.g., submersible bilge pump).
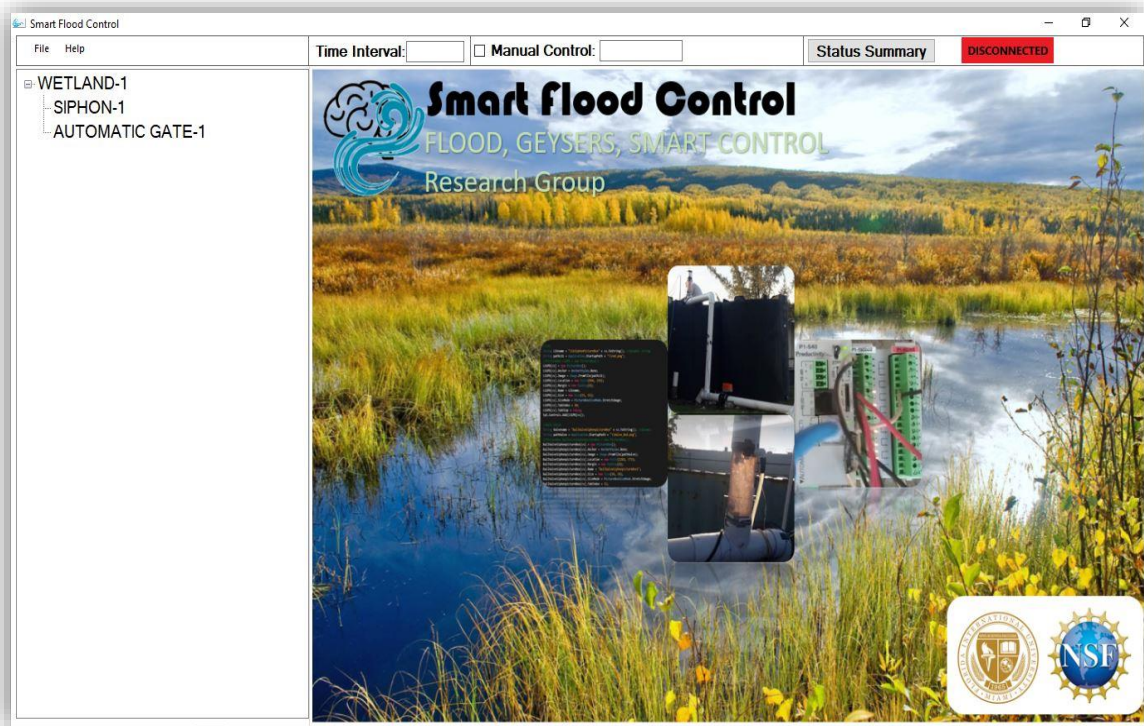
Figure 5. Main software interface for remote operation

As shown in Fig. 5, the interface summarizes the status (top right tab), where the system's overall status can be checked. The colors on the interface represent the operation status of the devices or the system. For the system, the green color indicates the normal functioning of all devices; the yellow color indicates that some components are not functioning, and the red color indicates that the entire system is not functioning. The Status Summary table is updated every 1 minute, but this interval can be changed as needed.

The Manual Control option allows the system to be operated manually. To open all actuated gates of a storage unit, the user will enter "1" in the box or "0" otherwise. These numbers can be used for multiple storage units. For instance, instruction 111000 indicates that all

11

actuated gates of storage units 1 to 3 will be opened, and those of storage units 4 to 6 will be closed or remain closed if they are in the closed position. Appendix B explains step by step procedure to set-up the software interface and the logic is explained as pseudo code in Appendix C.
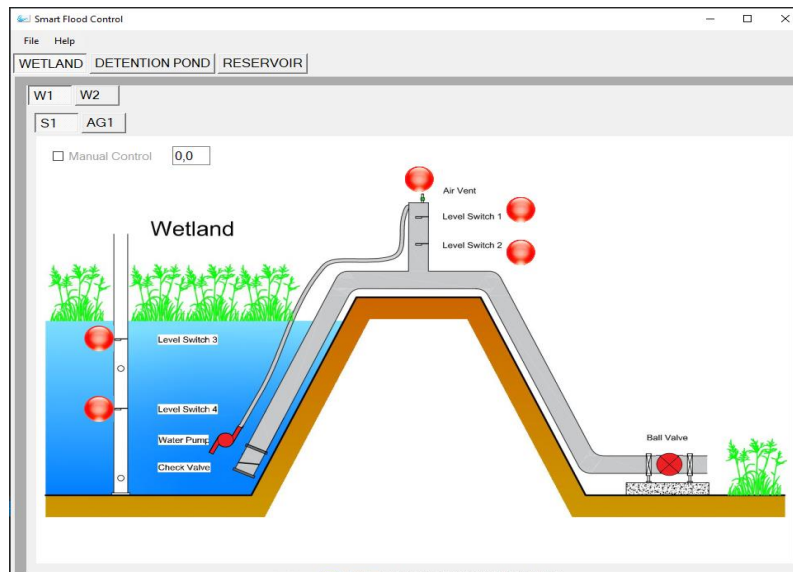
Figure 6. Software interface for remote operation of a siphon (S1)

2.3 Prototype setup, local and global connection

Fig. 7 shows a schematic of integrating the control software, communication, and siphon hardware. The process starts when the communication is established between the hardware employed in the lab and the control center (e.g., end-user). Once the communication has been established, the control center can operate the entire system manually or automatically.

All the hardware, water-level sensors, air vent, bilge pump, and actuated ball valve are connected to the PLC. The PLC is then connected via USB cable to the slave SDR,

connected to the master SDR remotely. A router that uses a 3G/4G cellular connection is employed to establish remote communication between the master SDR and the control center. All the devices are powered using a battery, which is recharged using a solar panel. The experimental results are illustrated in Appendix D.
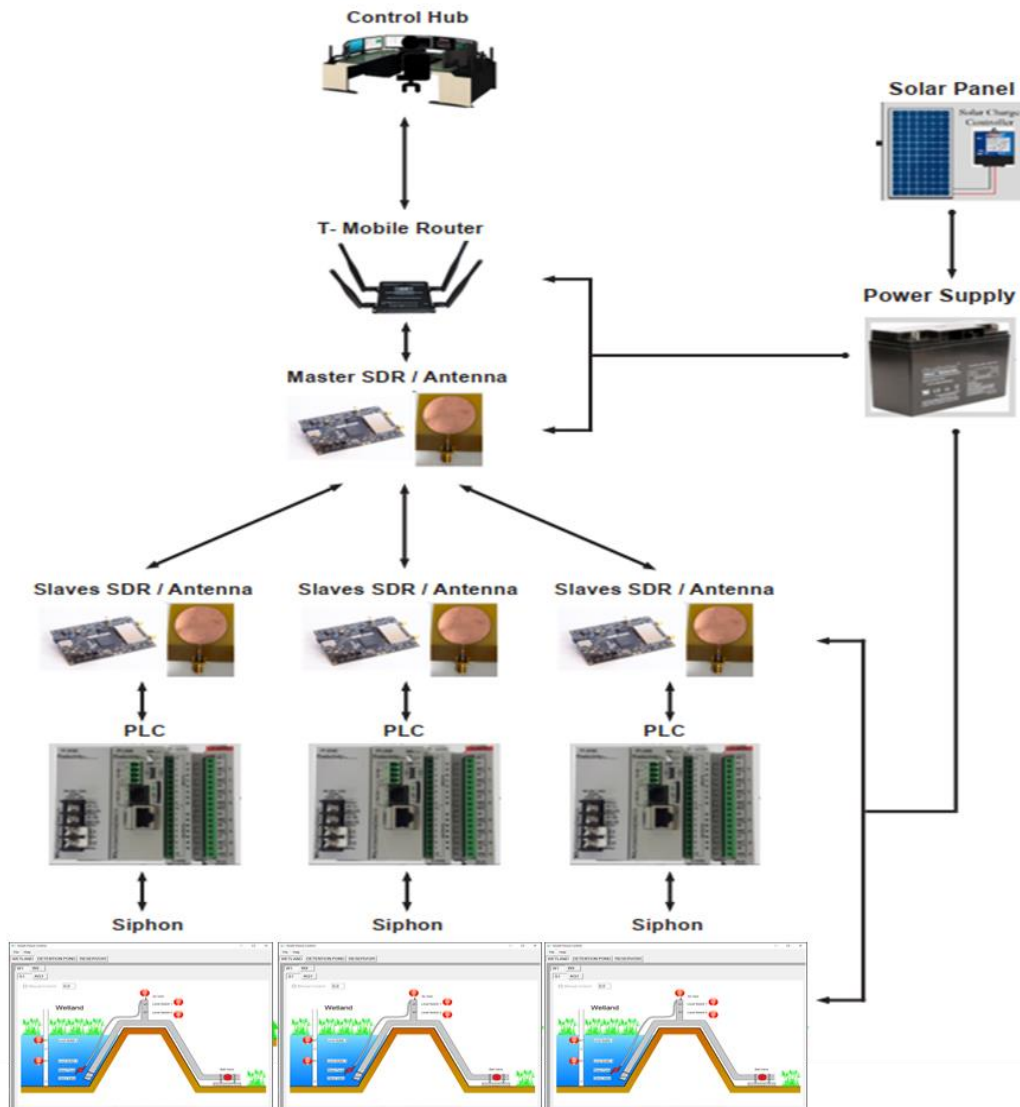
Figure 7. Schematic of the integration of the control software, communication, and the siphon hardware

2.3.1 Global communication

The schematic of global communication is explained in detail in the previous section and is illustrated in Fig. 7. The system operates as depicted in Fig. 7 when there is no connectivity problem, i.e., when the signal strength is good. However, when the connectivity is lost due to poor connection, the connection between the control hub and the Master SDR is lost, and the system stops functioning. To resolve this issue and make the system more reliable, a local connection is developed that is explained below.

2.3.2 Local communication

When the global connection is lost due to poor connectivity or other reasons, the proposed architecture establishes local communication between the PLCs and SDRs. The local communication is achieved with the help of algorithms deployed in SDRs, as depicted in Table 1 of section 2. The algorithm has been developed using open-source GNURadio and Python 2.7. The signal strength between the PLCs and SDRs is computed using a bit error rate (BER). The BER comes out to be less than 10-3, which is well within the accepted industry standard.

The algorithm establishes two-way communication between the sensors and the SDR via PLC. The data is read from sensors and then transmitted to the SDR via PLC. The SDR analyzes the input collected from sensors and provides the output to PLC, which operates the hardware such as water pump, actuated ball valve, and air vent. As proof of concept, several experiments have been performed in the RFCOM Lab at Florida International University (FIU) to verify the same.

2.4 Assumptions and Limitations

The proposed is based on the following assumptions:

1. One of our assumptions is that the siphon system is without any leakage. However, this needs to be carefully checked because the system is made by fitting different components such as water level sensors, air vent, and the bilge pump's pipe into the clear PVC pipe of the siphon system.

2. The siphon system can work for a water level head of 10 meters theoretically. Our system is about 2.5 meters from the ground, and we got good results. However, certain experiments have to be performed for three, four, five meters and so on to check the functioning of the siphon system.

3. The experimental results of the siphon system for the Miami region, which is mostly hot and humid, are almost the same. Therefore, we can conclude that the proposed siphon system works well. However, it should be check experimentally for other climatic conditions.

The limitations of the proposed system are as follows:

1. The siphon needs to be perfectly sealed at the negative pressure part. If there is any leakage in the negative pressure part, the air will flow into the siphon. When the air volume reaches a certain amount, the siphon flow will stop.

2. To ensure the efficiency of draining water by using a siphon pipe, a certain amount of elevation difference between the water level in the wetland and the siphon outlet level is required. Therfore, the siphon system won't work in those area where the topography is flat. This could limit the application of the siphon system.

CHAPTER 3: ARCHITECTURE FOR REMOTE CONTROL OF WATER RELEASE IN A NETWORK OF STORAGE UNITS USING INTERNET OF THINGS

3.1 Overview of the integrated platform for remote operation

As shown in Fig. 8, the integrated platform for remote operation can be represented by five-tier architectures consisting of User/Decision Support System (DSS), Virtual Private Network (VPN), micro-controller such as raspberry pi, PLC, and devices employed in the field such as water level sensors, bilge pump, air-vent, and actuated ball valve.
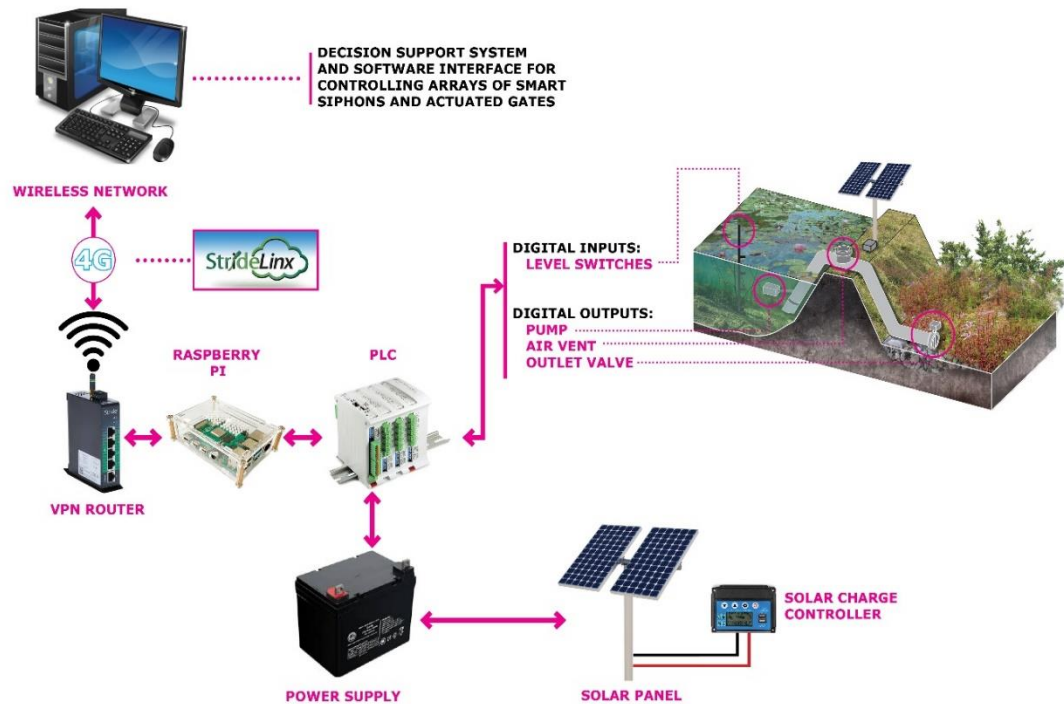
Figure 8. Schematic overview of integrated platform for remote operation

The first tier consists of devices employed in the field such as water level sensors, bilge pump, air-vent, and actuated ball valve. These devices collect near real-time information from the field and send it to the PLC. The second tier consists of PLC, which collects the

field data and receives a command from the user/remote computer to operate installed devices in the field. The third tier consists of a micro-controller like raspberry pi, which collects the data from the PLC and transmits it to the user/remote center via a VPN router. The fourth tier consists of a VPN router, which uses a 4G/5G cellular sim to provide internet connection between the user/remote center and the raspberry pi. Finally, the fifth tier consists of the user/remote center, which processes the data obtained from the field and commands the PLC to perform operations based on data received.

3.2 Hardware overview

Fig. 9 represents the schematic of hardware devices employed in this integrated platform. The hardware devices consist of liquid level switches, bilge pump, air-vent, and actuated butterfly valve.
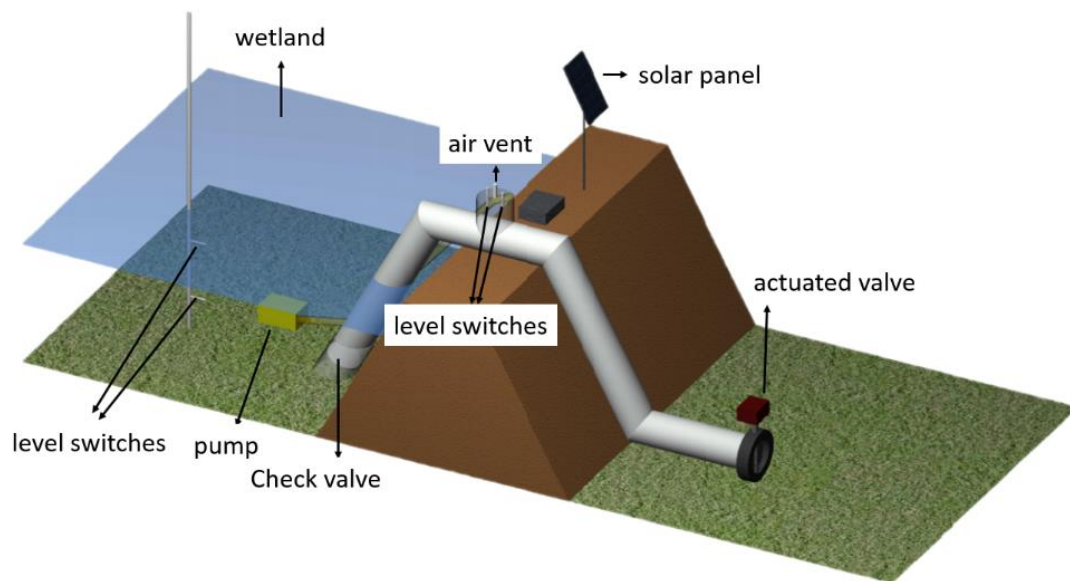
Figure 9. Schematic of hardware devices for the proposed integrated system

Description of the devices mentioned above are given below:

- VPN Router: A VPN router (Nighthawk 6-Stream AX5400 WiFi 6 Router (RAX50)) is employed to establish a connection between the raspberry pi and the user/remote center. It uses a 5 GHz radiofrequency and a WPA2-PSK security protocol.

- PLC: The Automationdirect Productivity 1000 CPU is employed in the proposed framework. It uses a 24 VDC power supply and consumes 5W. Additional input/output module such as P1-15CDD2 is used, input ports are used to connect liquid level switches, and output ports are used to connect air-vent and bilge pump. An output relay module, P1-08TRS, is also used to connect actuated butterfly valve. Both of the modules, P1-15CDD2, and P1-08TRS, consume 1.5W. Appendix A provides information about PLC.

- Battery: A couple of batteries (CooPower CP12-70 12V 75Ah Sealed Lead Acid Battery) are used to power VPN, raspberry pi, PLC, water level sensors, bilge pump, air-vent, and actuated ball valve. The battery is charged using the solar panel.

- Solar Panel: A solar panel (12V 100W High-Efficiency Monocrystalline PV Module) is used with one 12Amp Pulse Width Modulation (PWM) charge controller. PWM charge controller ensures that the battery is not overcharged and prevents damage to the battery.

3.3 Integrated control software

The integrated control software is explained in detail in section 2.2.

3.4 Local and global communication

Fig. 8 illustrates the schematic overview of integrated platform for remote operation. Global communication is employed to transfer data from the devices used in the field to the control center, which processes it and communicates it back to the field to perform the required operations. The system works perfectly fine when there are no connectivity issues. But due to poor weather/cloudy season, the system faces connectivity issues and becomes paralyzed as it cannot take the command from the control center. This problem is resolved using local communication through raspberry pi.

The conditions of C# program, developed for the control center, are copied to the raspberry pi. So, when the global communication is lost between the PLC and control center due to connectivity issues or some other reason, raspberry pi takes charge of the situation and operates the system based on inputs received from the field devices. The raspberry pi is using the Raspbian operating system, and the conditions are installed using python script.

The program has been developed in such a way that when the global communication is lost, the program switches itself and operates using local communication. When the strength of the signal return, the program automatically starts communicating using the global connection.

For some reason, even if the local communication is also not working, then the PLC will close all the siphon hydraulic system valves, bilge pump, and the air vent. The PLC is coded with the help of the ladder logic program installed using Productivity Suite software.

3.5 Comparison with SCADA system

The proposed integrated hardware and software architecture is analogous to the SCADA system as both of them employs collection, transmission, and control mechanism as their primary elements. The architecture of the control system LAN of the SCADA system is shown in Fig. 10 (Stouffer et. al, 2015). The proposed integrated hardware and software architecture employs Microsoft Azure IoT technology whose architecture is shown in Fig. 11.
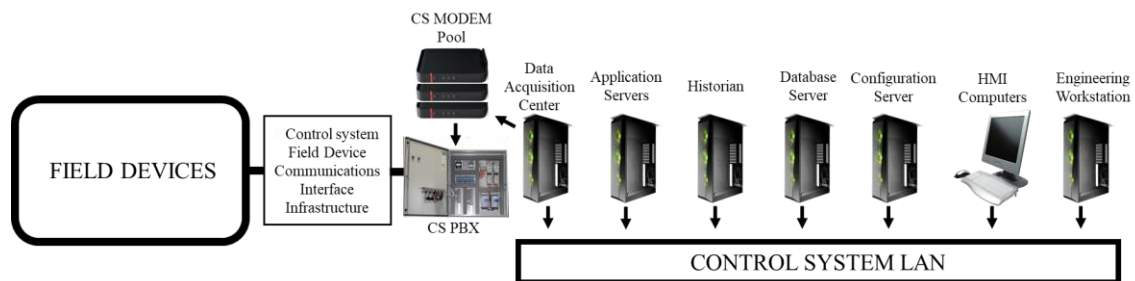
Figure 10. Architecture of control system LAN of the SCADA system
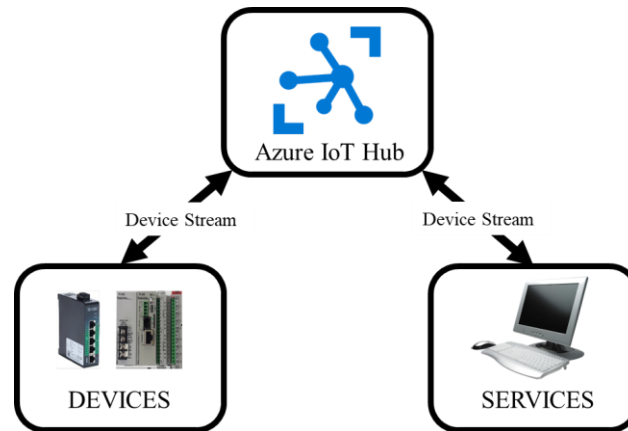
Figure 11. Architecture of Microsoft Azure IoT technology

The left side Fig. 10 shows the sensors/other devices collect data which is then transmitted to the controller/RTU/PLC/IED. The control system collects the data from the controller and pass it to the modem pool. It then goes to several servers such as data acquisition, application, database, configuration and finally to the engineering workstation. The entire set of servers are known as Control System LAN. The data is being processed at the engineering workstation and via same communication channel it reaches back to sensors/other devices.

As shown in Fig. 11, the sensors/devices collect data and transmit it to the Azure IoT Hub. The transmission is achieved using router that employs 4G/5G sim to provide internet connection. The IoT hub is connected to the remote computer via one of the services known as IoT cloud. Thus, the data reaches from field to the remote computer and is processed and send it back to the devices via the same channel as shown in Fig. 11.

As seen from Fig. 10, the SCADA systems are composed of several modules that perform various functions, which may become overburdened at times. This integrated module system increases the cost of the SCADA system. Also, because the system is complicated, trained operators, analysts, and programmers are required to maintain the SCADA system. SCADA systems are routinely updated to add or alter tags, units of measurement, scripts, alert thresholds, and synoptic. This implies that SCADA programs must be restarted often. In terms of hardware components and dependent modules, a PLC-based SCADA system is complicated. Fig. 11 shows the working architecture of the Microsoft Azure IoT technology, which uses a relatively simpler system. The data is being sent using a single server, hence reducing the complexity and cost associated with the system.

One of the major limitations of the SCADA system is that it can be used to operate only one siphon system. Therefore, a new software interface is designed and developed to operate and monitor multiple siphon systems. Moreover, the program has been developed in such a way that it can operate multiple components of a single system. For instance, more than one level switches can be monitored using the proposed siphon system; however, the SCADA system can monitor only one level switch. This incorporates the operational reliability of the proposed system compared to the existing SCADA system.

3.6 Operational reliability assessment of reliability block diagram model using ExtendSim

Reliability block diagram (RBD) has been widely and extensively used in reliability engineering (Guo and Yang, 2007). All the components in the system are connected by graphic blocks following their functional logic or operational relationship. Therefore, a

complex system becomes intuitive and easy to build and read in RBD (Distefano and Xing, 2006; Wang et al., 2004). However, RBD was only used for non-repairable systems (Distefano and Puliafito, 2007; Rausand and Høyland, 2003). Because of this limitation, the reliability module based on ExtendSim software has been developed by the Imagine that Inc. Company to achieve RBD application for both repairable and non-repairable systems. On ExtendSim software, a reliability model is built by different functional blocks stored in the Reliability Library. As a result, the ExtendSim RBD can simulate complex systems' maintenance processes in addition to its intuitive and user-friendly advantage. By applying the Monte Carlo simulation method, the ExtendSim RBD model can provide accurate results for the system's operational reliability.

In the RBDs, each graphic block represents one physical component in the system with an associated mathematical function or a simulation model. There are only two possible working states for all the components, a functioning state (UP) and a failed state (DOWN), which can be described as equation (1).

$$X(t) = \begin{cases} 1 & \text{if the component is functioning at time t} \\ 0 & \text{if the component is not functioning at time t} \end{cases} \tag{1}$$

The two-parameter Weibull distribution is applied in this study to simulate all the components' lifetime distribution due to its flexibility and widespread application in the reliability engineering industry (Fu et al., 2019; Zhang and Xie, 2007).

Assume that a component enters in operation at time t = 0 and the time to failure (TTF) T is continuously distributed with the probability density function of $t \sim \text{Weibull}(a, \frac{1}{\lambda})$, $\frac{1}{\lambda} =$

β, where, a is the shape parameter, and β or $\frac{1}{\lambda}$ is a scale parameter, also called characteristic lifetime.

$$f(t) = \begin{cases} a\lambda^a t^{a-1} e^{-(\lambda t)^a} & for\ t > 0 \\ 0 & otherwise \end{cases} \tag{2}$$

The probability of the component failing within the time interval $(0, t)$ can be described by Equation (3).

$$F(t) = Pr(T \leq t) = \int_0^t a\lambda^a x^{a-1} e^{-(\lambda t)^a} dx = 1 - e^{-(\lambda t)^a} \tag{3}$$

Thus, the reliability of the component can be described by Equation (4)

$$R(t) = 1 - F(t) = e^{-(\lambda t)^a} \tag{4}$$

The above equation presents the operational reliability, which indicates the probability that a system is functioning adequately over any given time (Chen et al., 2013).

Maintenance actions enhance the performance of a system within acceptable limits. Maintenance in this study is limited to replace one or more broken components in the system with new ones. Now assume the time to maintain $T_m = (T_{m1}, T_{m2}, \cdots, T_{mn})$, the general f(t) with the application of maintenance is updated as shown below

$$f^*(t) = \begin{cases} f(t) & ,\ t < T_{m1} \\ f(t - T_{mi}) \cdot \prod_{j=1}^{i} R_s(T_{mj} - T_{mj-1}) & ,\ T_{mi} \leq t < T_{mi+1}, i \geq 1 \end{cases} \tag{5}$$

The above equation is integrated to obtain a general version of R(t)

$$R_s^*(t) = \begin{cases} R_s(t), \ t < T_{m1} \\ R_s(t - T_{mi}) \cdot \prod_{j=1}^{i} R_s(T_{mj} - T_{mj-1}), \ T_{mi} \leq t < T_{mi+1}, i \geq 1 \end{cases} \qquad (6)$$

Where, $R_s^*(t)$ means maintenance for the entire system

By applying maintenance at regular intervals TM, the equation above becomes

$$R_s^*(t) = R_s(t - i \cdot TM) \cdot R_s(TM)^i, \ i \cdot TM \leq t \leq (i + 1) \cdot TM \qquad (7)$$

Equation (7) can be found in various references (Kececioglu, 2003; Klaassen and Peppen, 1990; Yang et al., 2006).

Components can be connected either in series or parallel in a system. Series components are the main components that must work in order to run the siphon system. The siphon system's operational reliability can be enhanced with the help of redundancy, i.e., the addition of parallel components to the series components.

In system engineering, redundancy is often expressed as N+K, where N is the minimum number of units required by the system to work, and K is the number of redundant units. In the proposed architecture of the remotely controlled siphon system, only one series component is required for the system to work; therefore, N is always equal to one, as shown in Fig. 12 (a). The redundancy of one (K=1), two (K=2), and three (K=3) for components L.S., B.P., and A.V. are shown in Fig. 12 (b), (c), and (d), respectively.
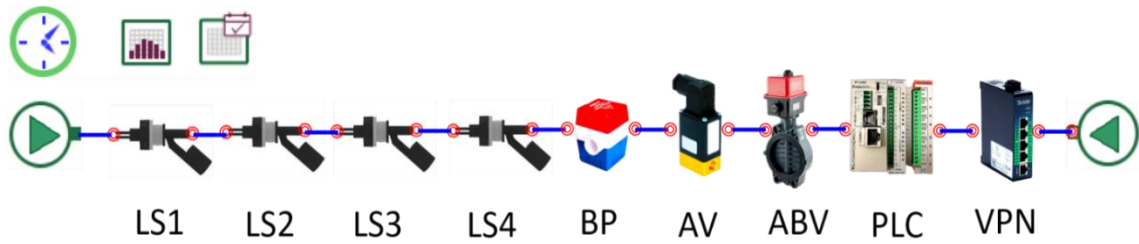
Scenario 1 (S1): Redundancy = 0 (N1+K0)
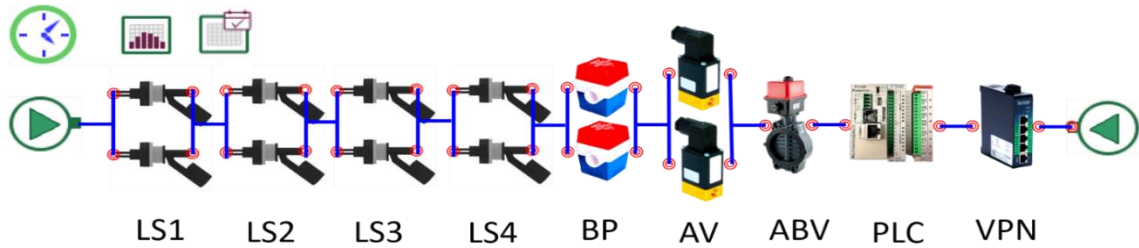
(b) Scenario 2 (S2): Redundancy = 1 (N1+K1)
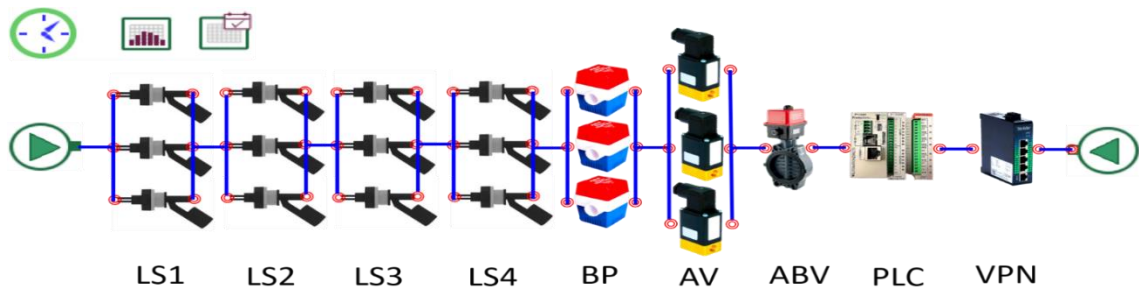
(c) Scenario 3 (S3): Redundancy = 2 (N1+K2)
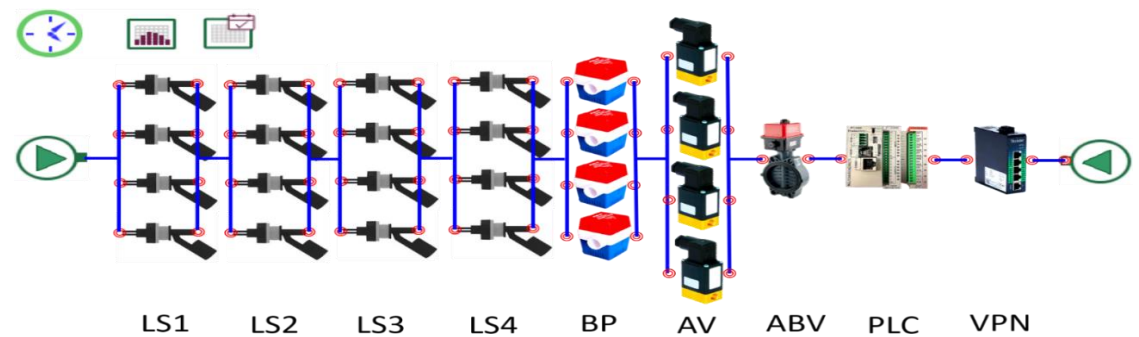
(d) Scenario 4 (S4): Redundancy = 3 (N1+K3)

Figure 12. Four scenarios of the siphon system using RBD functional blocks

The maximum number of redundancies that can be achieved depends on pipe diameter. A six-inch diameter pipe is used in the proposed system, for which maximum redundancy comes out to be three. The redundancy can be further increased by increasing the pipe diameter. Table 2 illustrates the same four scenarios of Fig. 12 in a concise form employed in the RBD model. In Table 2, LS1 stands for level switch 1, LS2 stands for level switch 2, LS3 stands for level switch 3, LS4 stands for level switch 4, BP stands for bilge pump, AV stands for air vent, ABV stands for actuated butterfly valve, PLC stands for programmable logic controller, and VPN stands for virtual private network.

Table 2. Four scenarios of the siphon system in the RBD model

Scenario	Redundancy	LS1	LS2	LS3	LS4	BP	AV	ABV	PLC	VPN
S1	0	N1+K0	N1+K0	N1+K0	N1+K0	N1+K0	N1+K0	N1+K0	N1+K0	N1+K0
S2	1	N1+K1	N1+K1	N1+K1	N1+K1	N1+K1	N1+K1	N1+K0	N1+K0	N1+K0
S3	2	N1+K2	N1+K2	N1+K2	N1+K2	N1+K2	N1+K2	N1+K0	N1+K0	N1+K0
S4	3	N1+K3	N1+K3	N1+K3	N1+K3	N1+K3	N1+K3	N1+K0	N1+K0	N1+K0

CHAPTER 4: RESULTS AND DISCUSSION

To demonstrate the applicability of the new platform, a series of laboratory testings were performed at FIU. The lab setup of multiple 6-inch diameter siphon and conventional drainage pipe systems are illustrated in Fig. 13. The total length of the siphon pipe and conventional drainage pipe is approximately 25 feet and 15 feet, respectively. The capacity of the tank is 2,500 gallons with 90-inch in diameter and 98-inch in height. The flow discharge data has been acquired using the Omega FDT-40 transit time ultrasonic flow meter; meanwhile, the water level has been measured using Omega LVCN 414. Both instruments are connected to the NI-6323 data acquisition instrument through the SCB-64A terminal.
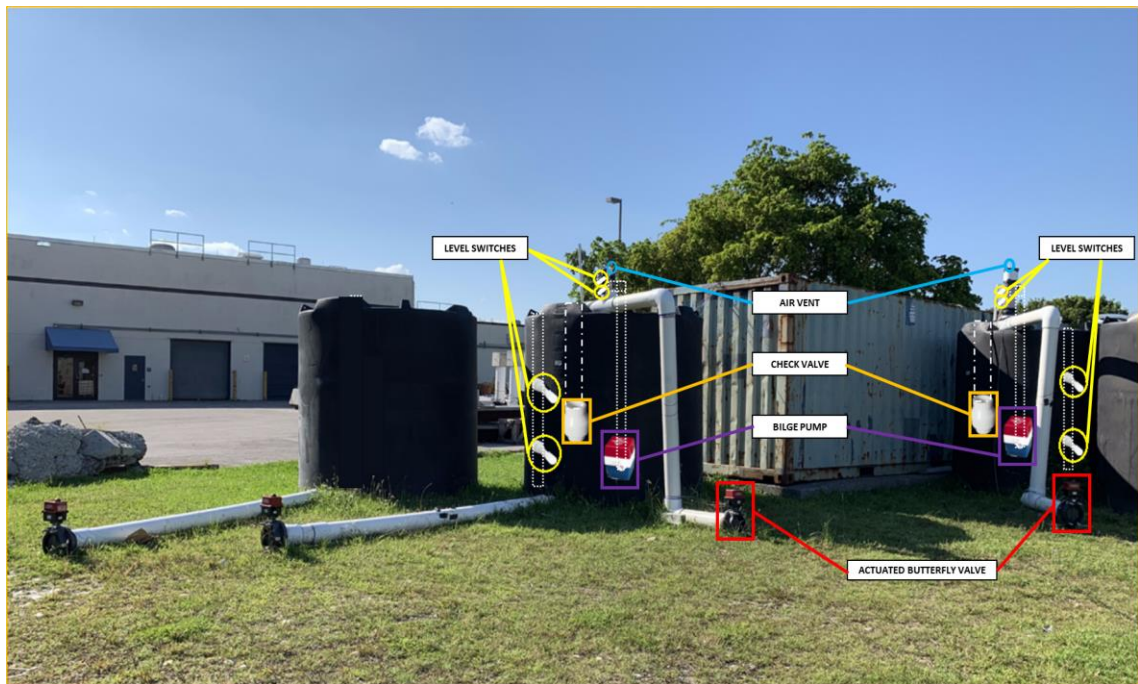
Figure 13. Lab setup of multiple siphons and conventional drainage pipe hydraulic systems

Several experiments have been performed in the lab at Florida Internal University (FIU) to check the proposed siphon system's functioning under different scenarios. Every scenario is performed multiple times to ensure the reproducibility of the experiments. Also, two different types of conditions of actuated ball valves are taken into consideration – one with a slow opening and the other with a fast opening. The following section presents the plots between the flow rate (L/sec) and the water depth (cm).

4.1 Experimental results and discussion

Fig. 14, 15, and 16 illustrate three experimental results with full capacity, i.e. when the tank is completely filled with water for the slow opening of the actuated ball valve. The vertical axis on the left represents flow rate in liter per second, and the vertical axis on the right represents water depth in cm. The flow rate is shown using the orange color, whereas water depth is illustrated in blue color. The horizontal axis signifies the time in seconds. Fig. 17 represents all the results of Fig. 14, 15, and 16 in a single plot.

Figure 14. Result of Experiment 1 for controlled siphon system with 100% initial water depth (6-inch diameter actuated butterfly valve)

Figure 15. Result of Experiment 2 for controlled siphon system with 100% initial water depth (6-inch diameter actuated butterfly valve)

Figure 16. Result of Experiment 3 for controlled siphon system with 100% initial water depth (6-inch diameter actuated butterfly valve)

Figure 17. Result of Experiment 1, 2, and 3 for controlled siphon system with 100% initial water depth (6-inch diameter actuated butterfly valve)

Fig. 18, 19, and 20 illustrate three experimental results with 75% capacity of the water tank completely filled with water with the actuated ball valve's slow opening condition. Fig. 21 represents all the results of Fig. 18, 19, and 20 in a single plot.

Figure 18. Result of Experiment 1 for controlled siphon system with 75% initial water depth (6-inch diameter actuated butterfly valve)

Figure 19. Result of Experiment 2 for controlled siphon system with 75% initial water depth (6-inch diameter actuated butterfly valve)

Figure 20. Result of Experiment 3 for controlled siphon system with 75% initial water depth (6-inch diameter actuated butterfly valve)

Figure 21. Result of Experiment 1, 2, and 3 for controlled siphon system with 75% initial water depth (6-inch diameter actuated butterfly valve)

Fig. 22, 23, and 24 illustrate three experimental results with 50% capacity of the water tank completely filled with water with the actuated ball valve's slow opening condition. Fig. 25 represents all the results of Fig. 22, 23, and 24 in a single plot.

Figure 22. Result of Experiment 1 for controlled siphon system with 50% initial water depth (6-inch diameter actuated butterfly valve)

Figure 23. Result of Experiment 2 for controlled siphon system with 50% initial water depth (6-inch diameter actuated butterfly valve)

Figure 24. Result of Experiment 3 for controlled siphon system with 50% initial water depth (6-inch diameter actuated butterfly valve)

Figure 25. Result of Experiment 1, 2, and 3 for controlled siphon system with 50% initial water depth (6-inch diameter actuated butterfly valve)

Similarly, experiments have been performed with the actuated ball valve's fast opening condition under three scenarios, first with full capacity, second with 75% of the capacity, and last with 50% capacity of the water tank. Fig. 26, 27, and 28 represent the result of the three trials for the water tank's full capacity. Fig 30, 31, and 32 represents the result of the three trials for 75% capacity of the water tank. Fig. 34, 35, and 36 represent the three trials for 50% capacity of the water tank. Fig. 29, 33, and 37 represent three trial results in a single plot with full capacity, 75% capacity, and 50% capacity of the water tank.

Again, the vertical axis in the left represents flow rate in liter per second, and the vertical axis in the right represents water depth in cm. The flow rate is shown using the orange color, whereas water depth is illustrated in blue color. The horizontal axis signifies the time in seconds
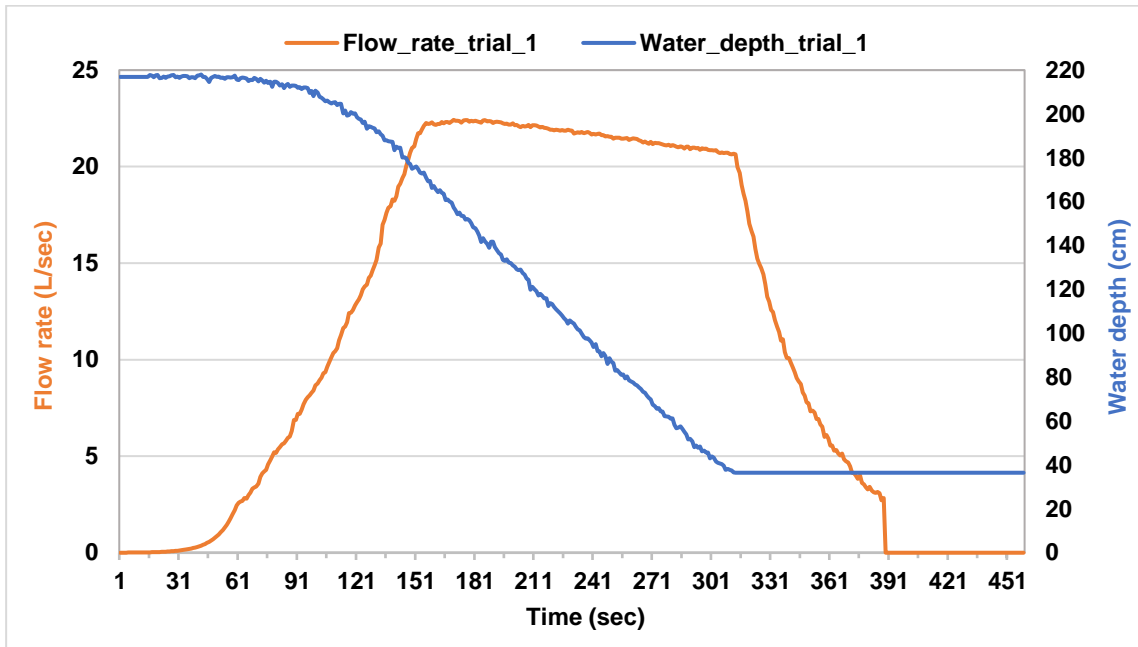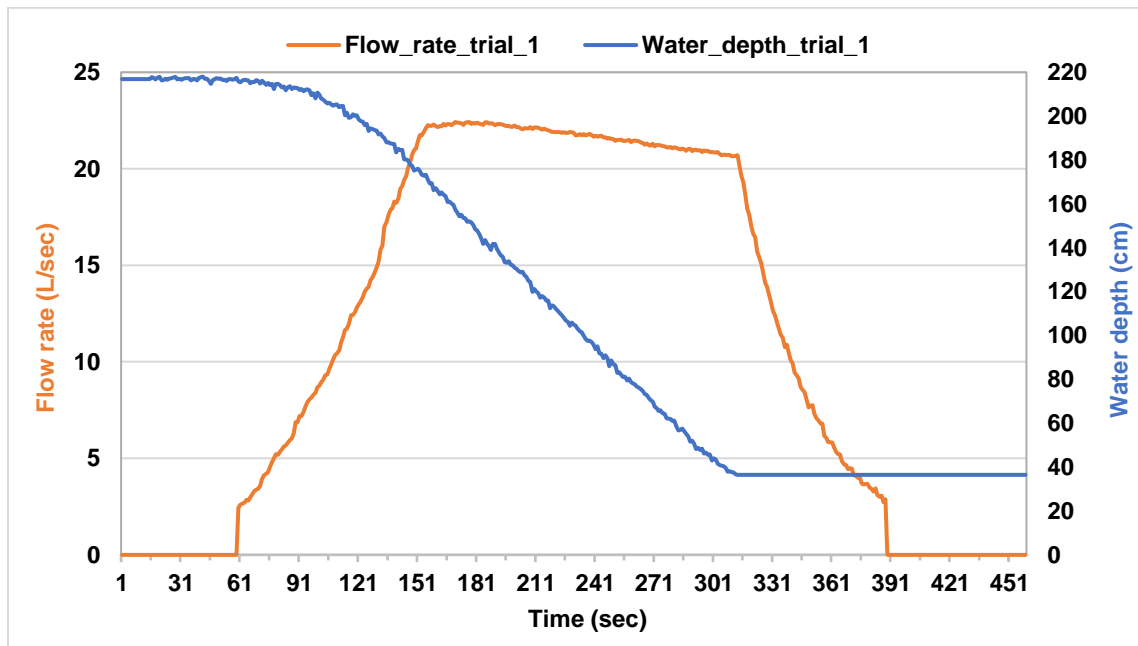

Figure 26. Result of Experiment 1 for controlled siphon system with 100% initial water depth (6-inch diameter actuated butterfly valve)
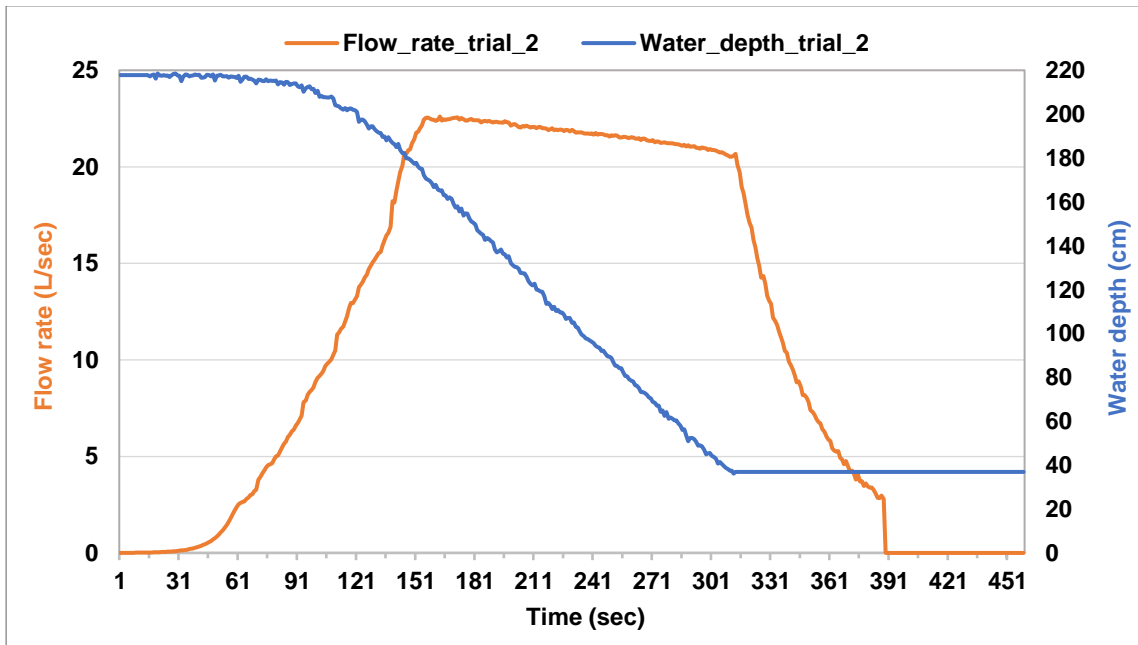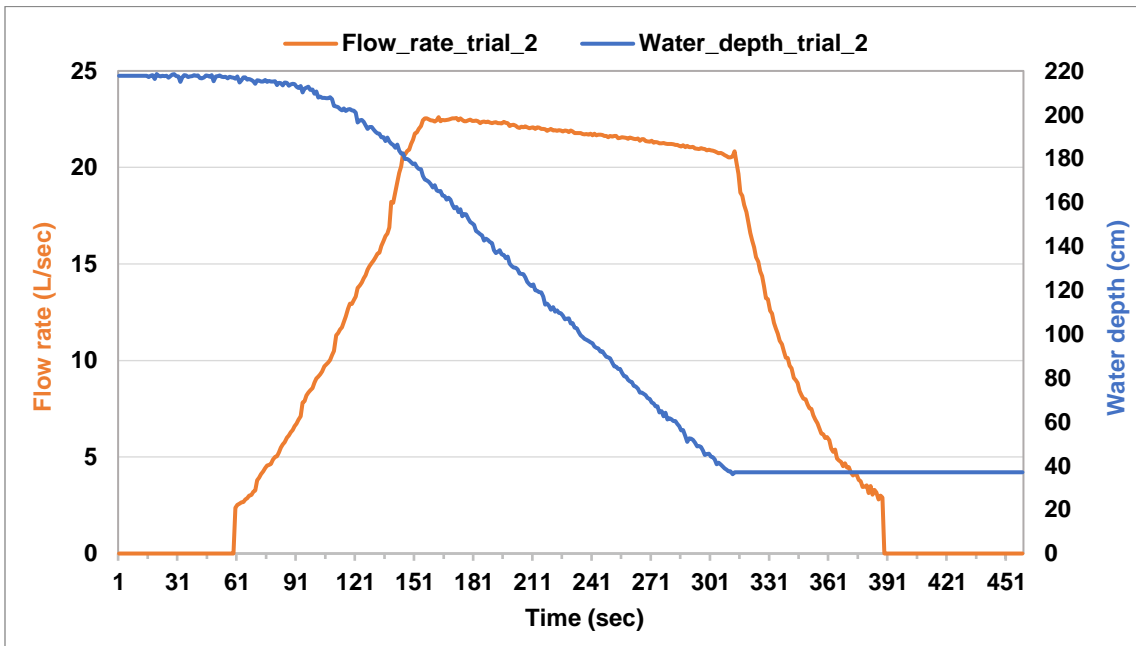
Figure 27. Result of Experiment 2 for controlled siphon system with 100% initial water depth (6-inch diameter actuated butterfly valve)
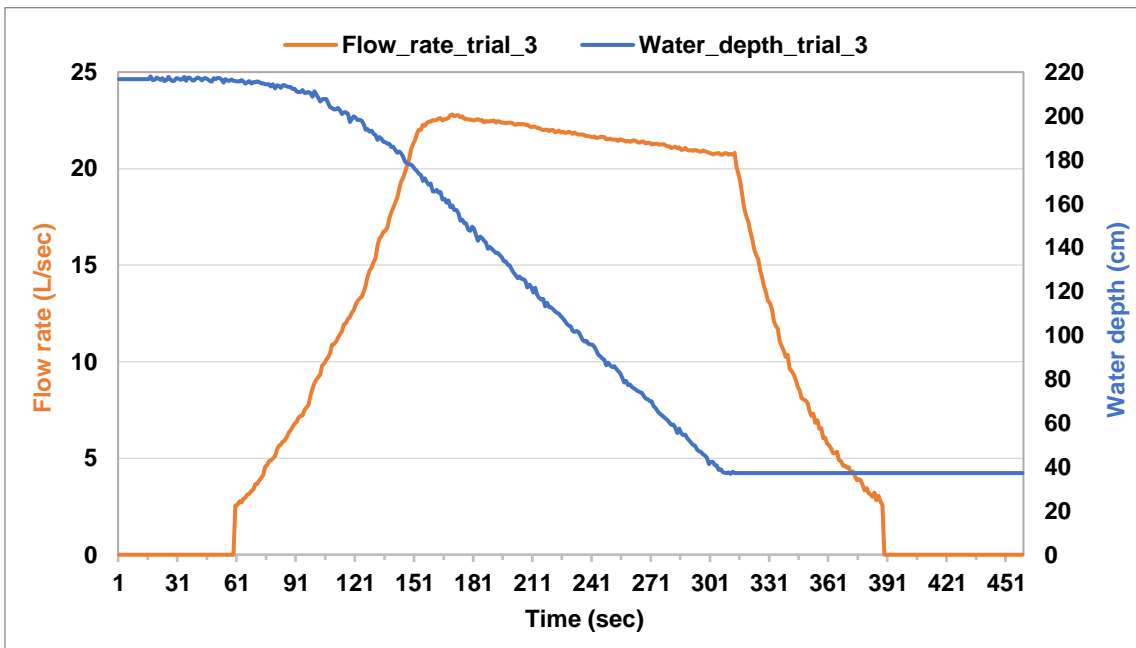
Figure 28. Result of Experiment 3 for controlled siphon system with 100% initial water depth (6-inch diameter actuated butterfly valve)
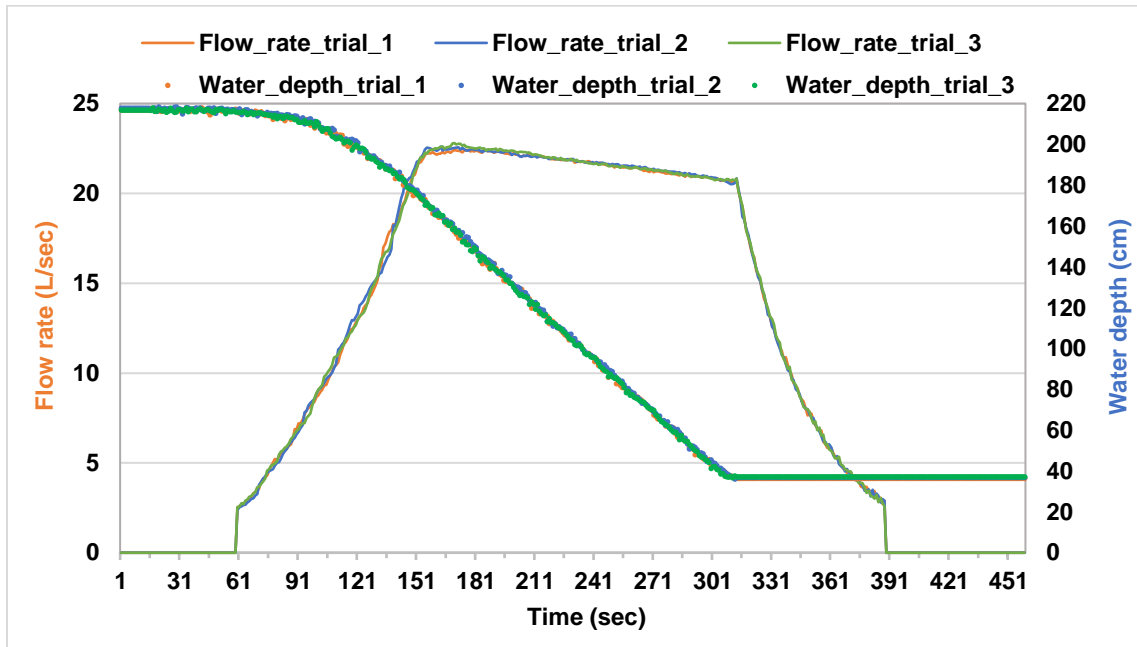
Figure 29. Result of Experiment 1, 2, and 3 for controlled siphon system with 100% initial water depth (6-inch diameter actuated butterfly valve)

As the actuated ball valve has a fast-opening condition, sudden increase and drop are seen at the starting and end of the experiment, i.e., when the ball valve opens and closed, respectively.
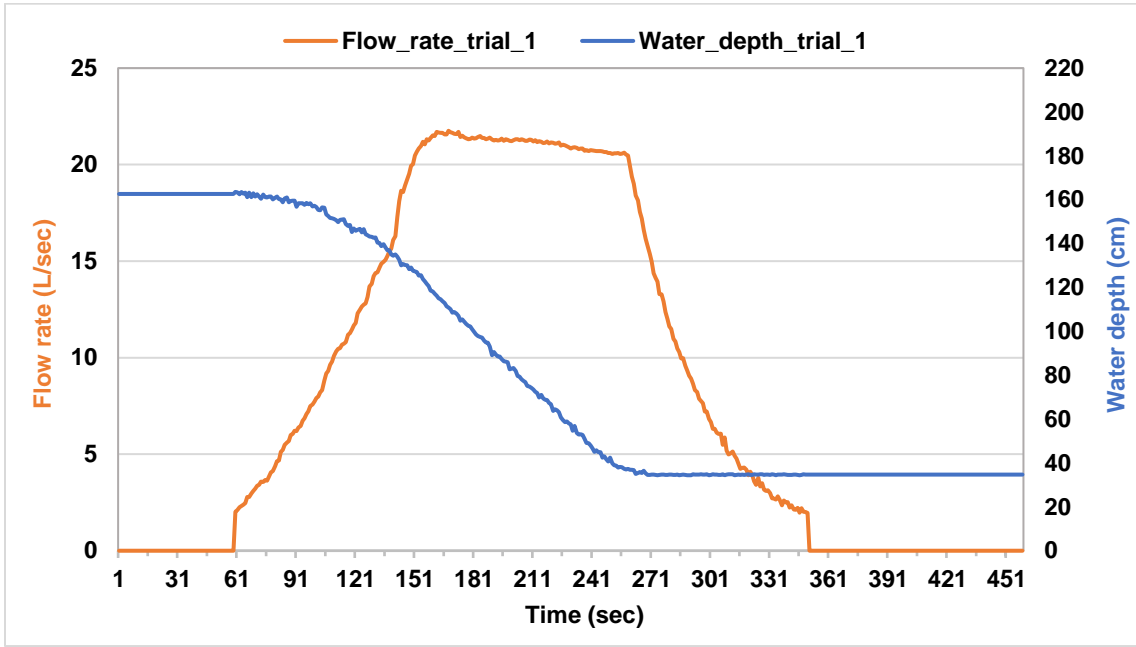
Figure 30. Result of Experiment 1 for controlled siphon system with 75% initial water depth (6-inch diameter actuated butterfly valve)
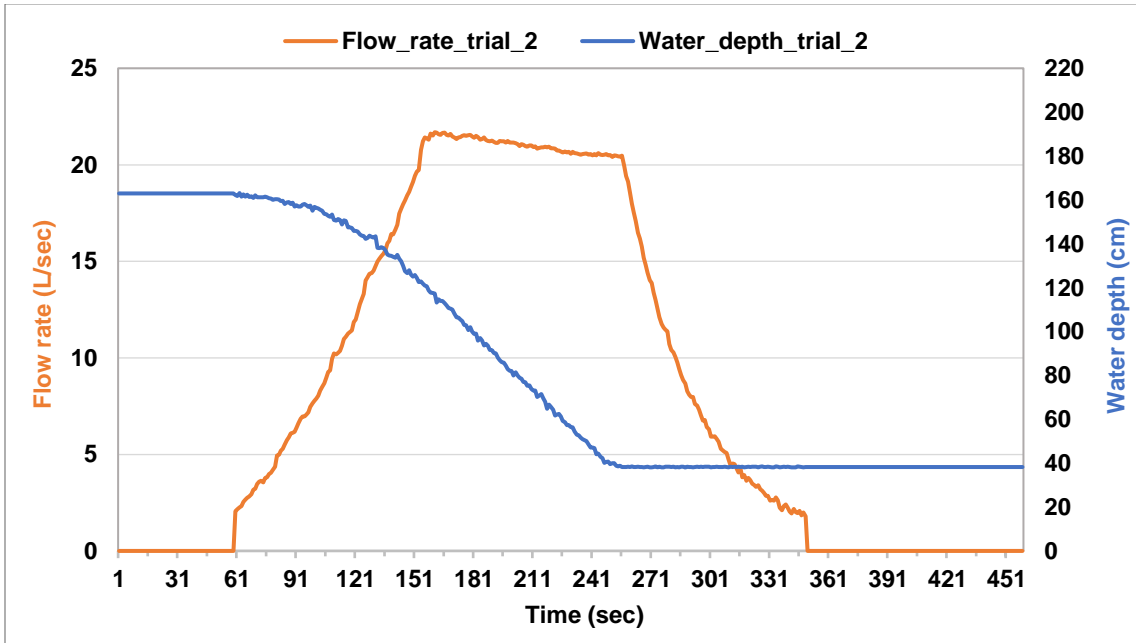
Figure 31. Result of Experiment 2 for controlled siphon system with 75% initial water depth (6-inch diameter actuated butterfly valve)
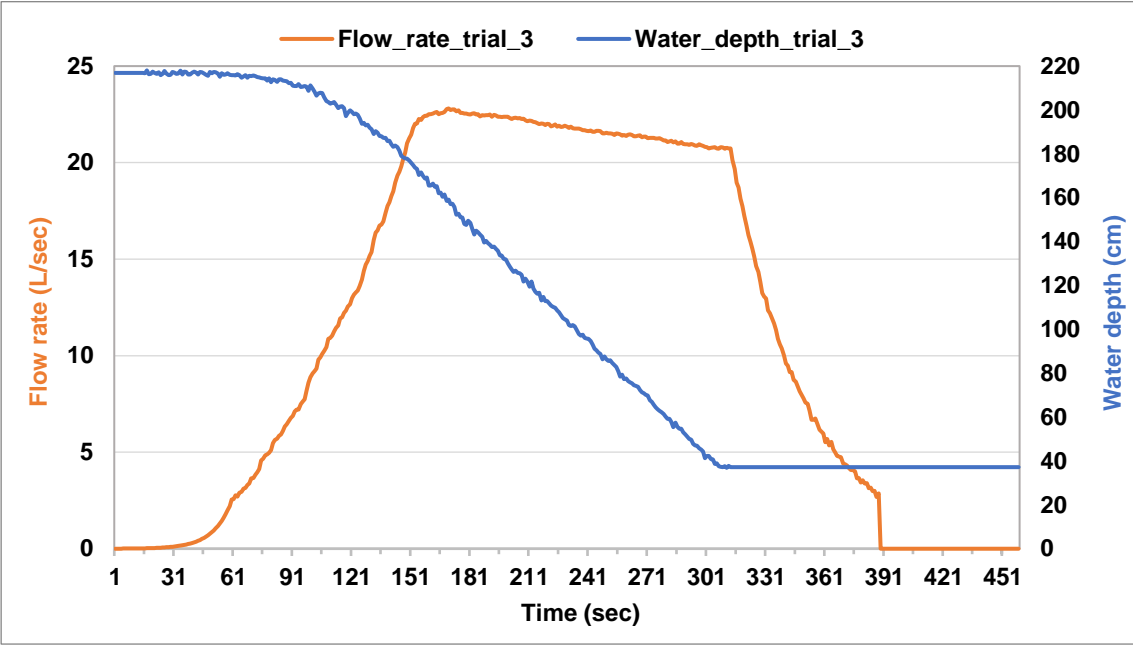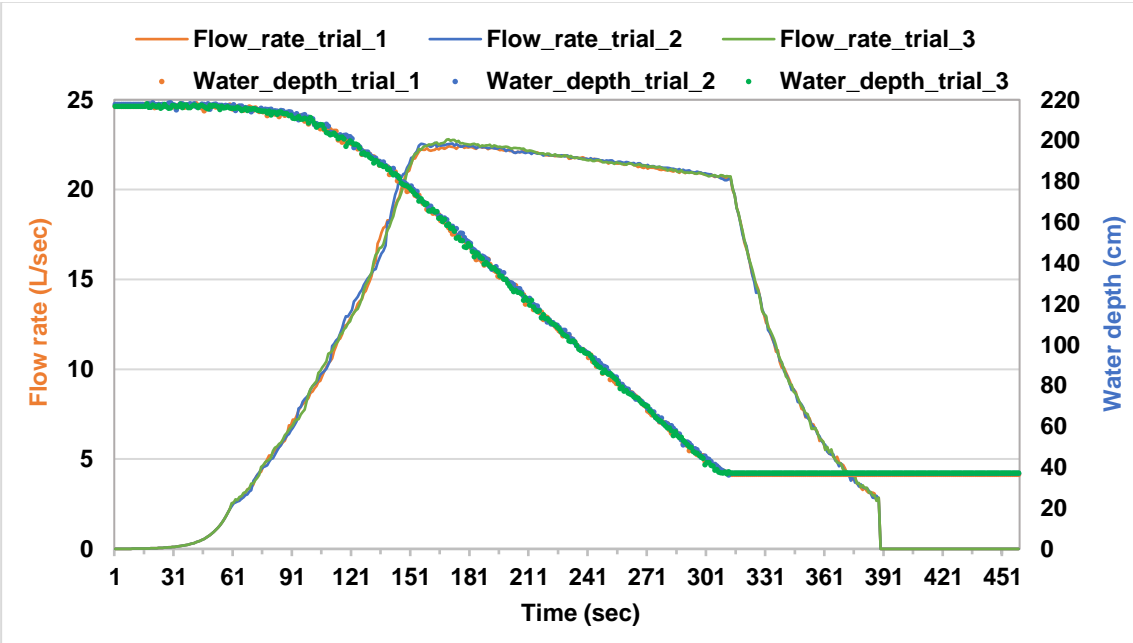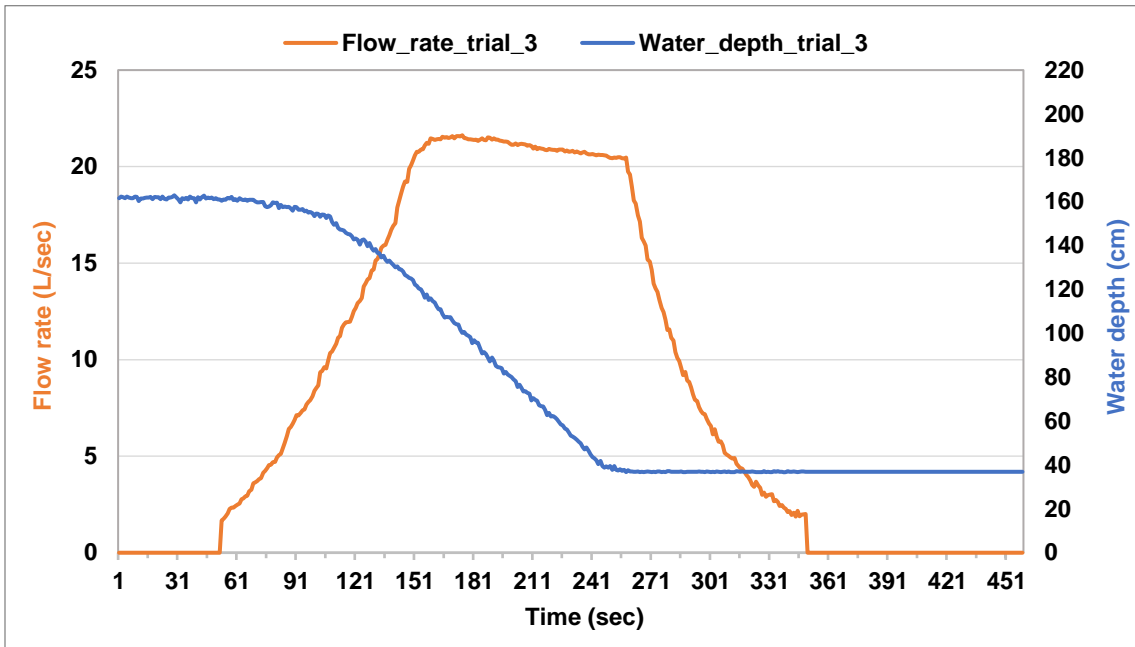
Figure 32. Result of Experiment 3 for controlled siphon system with 75% initial water depth (6-inch diameter actuated butterfly valve)
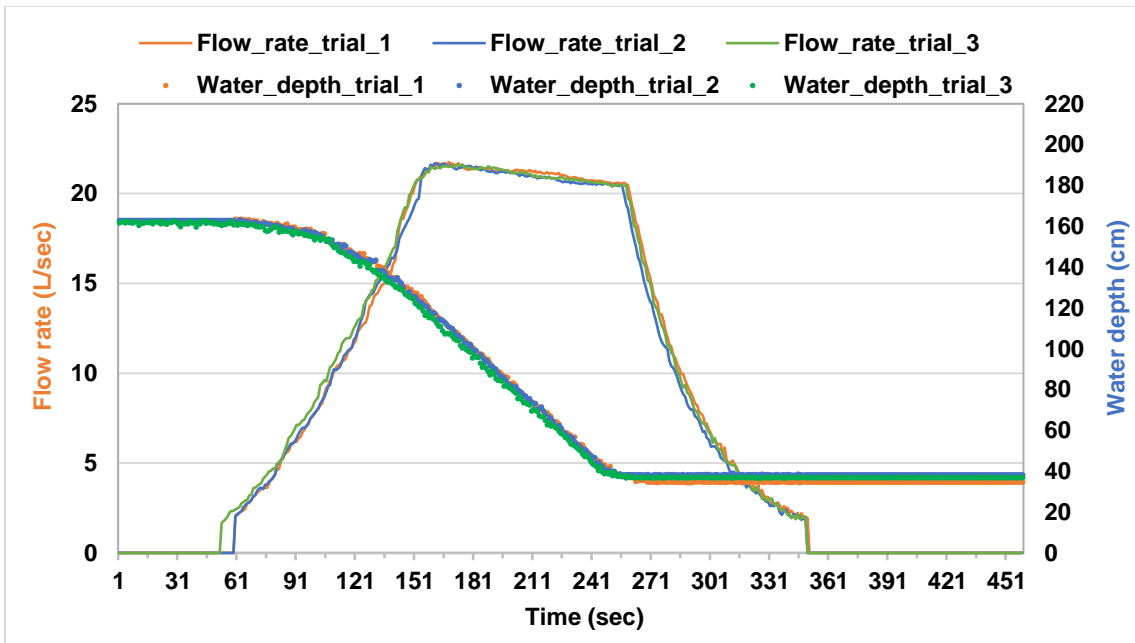
Figure 33. Result of Experiment 1, 2, and 3 for controlled siphon system with 75% initial water depth (6-inch diameter actuated butterfly valve)
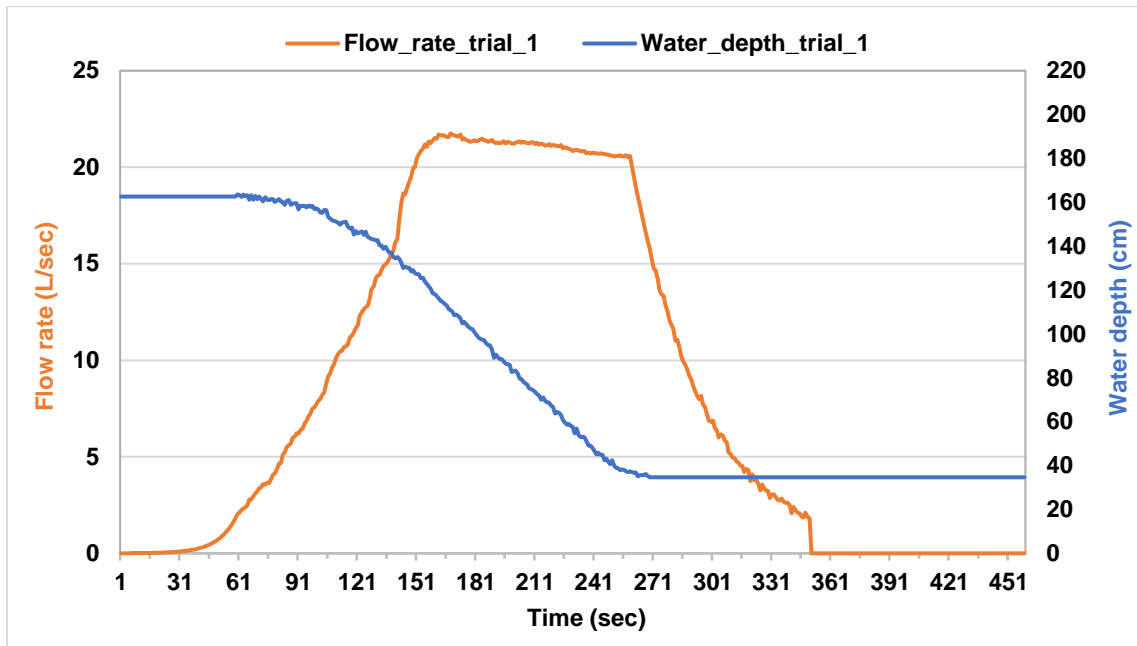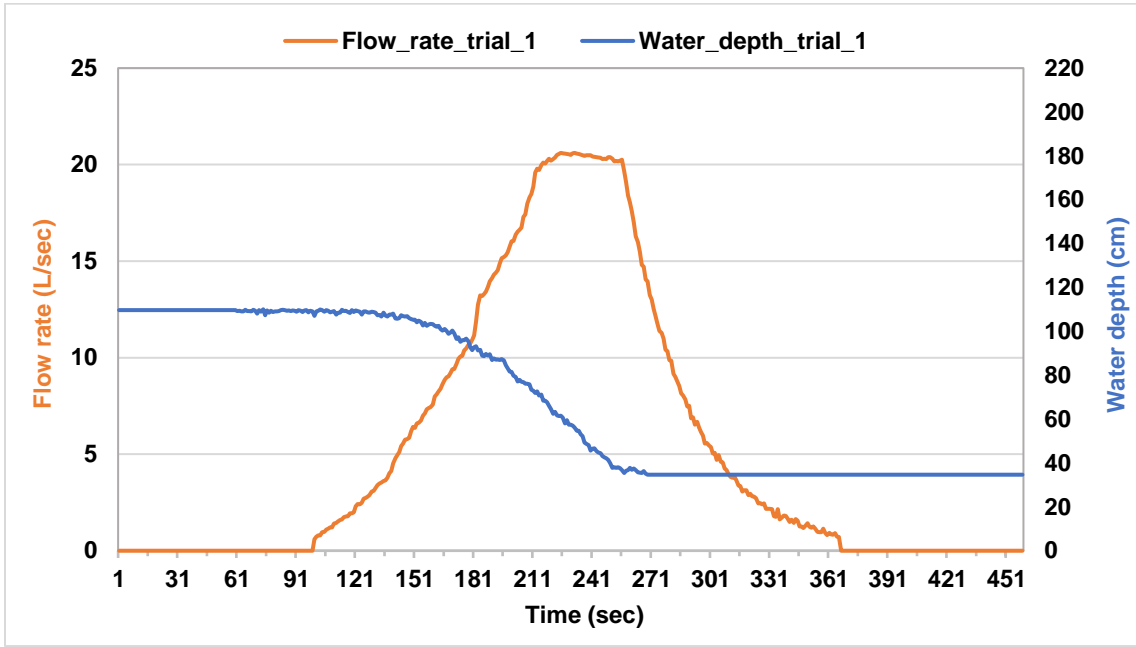
Figure 34. Result of Experiment 1 for controlled siphon system with 50% initial water depth (6-inch diameter actuated butterfly valve)
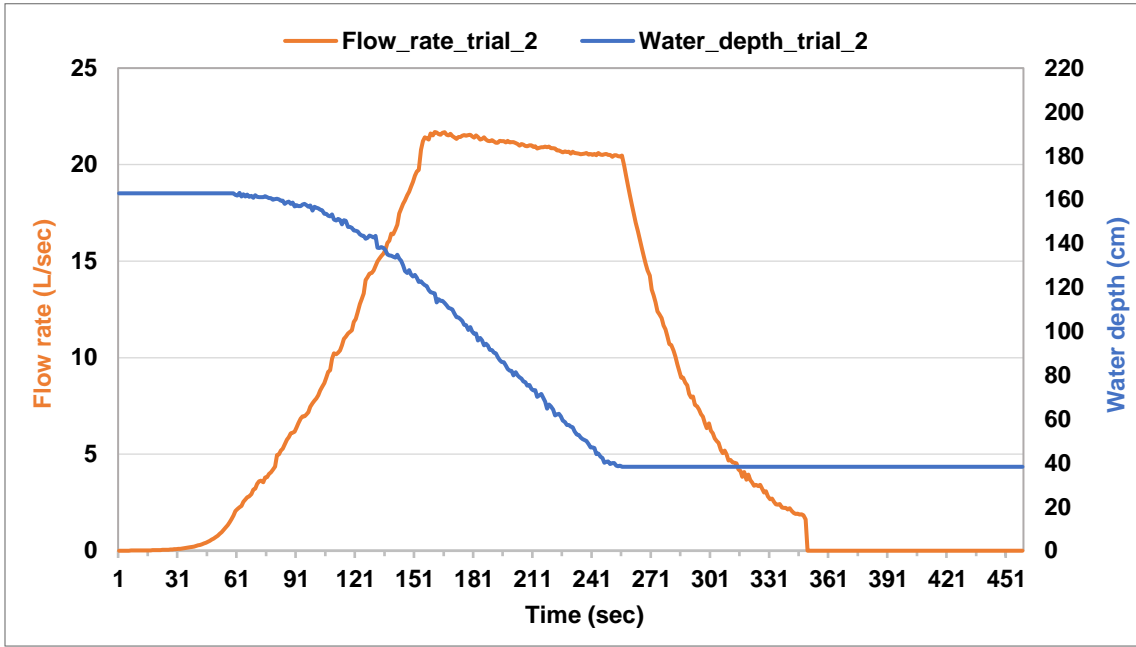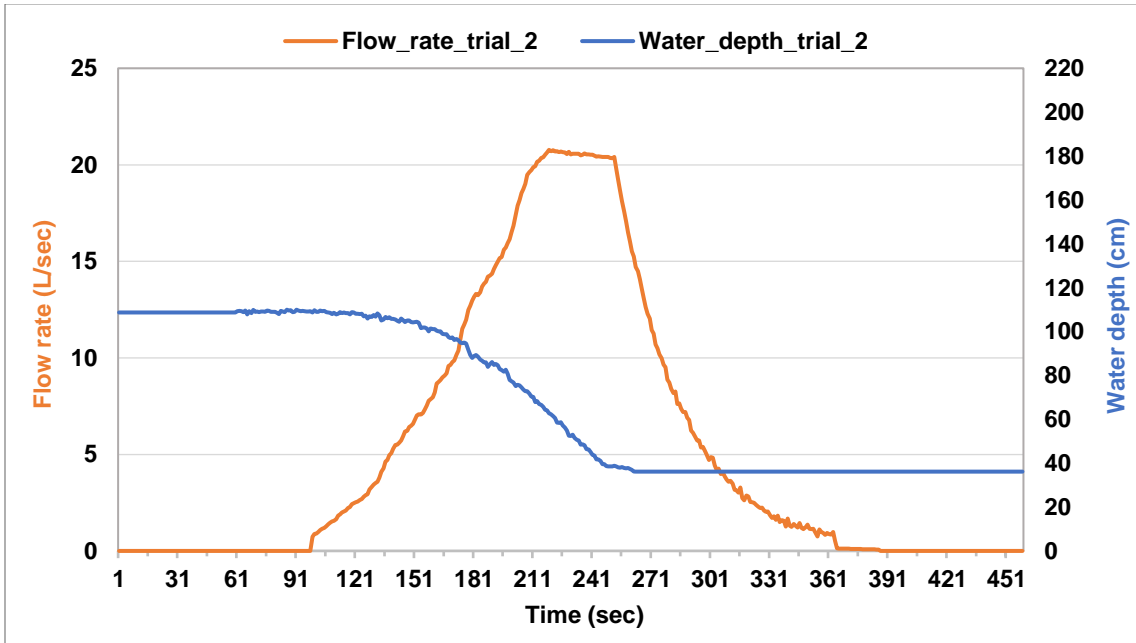

Figure 35. Result of Experiment 2 for controlled siphon system with 50% initial water depth (6-inch diameter actuated butterfly valve)
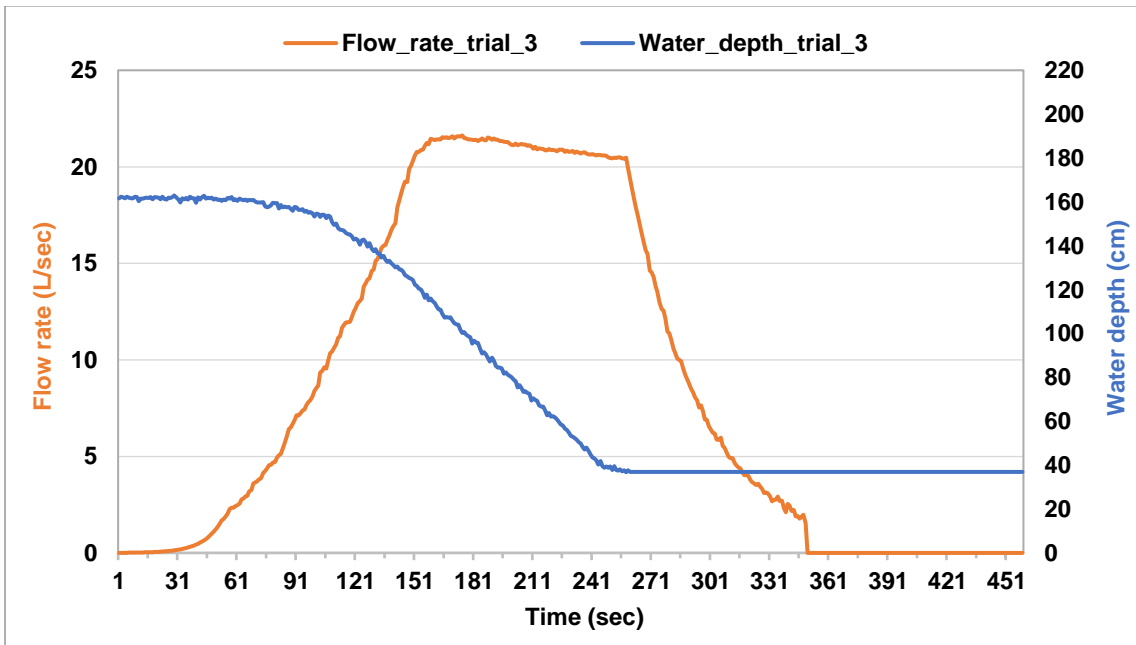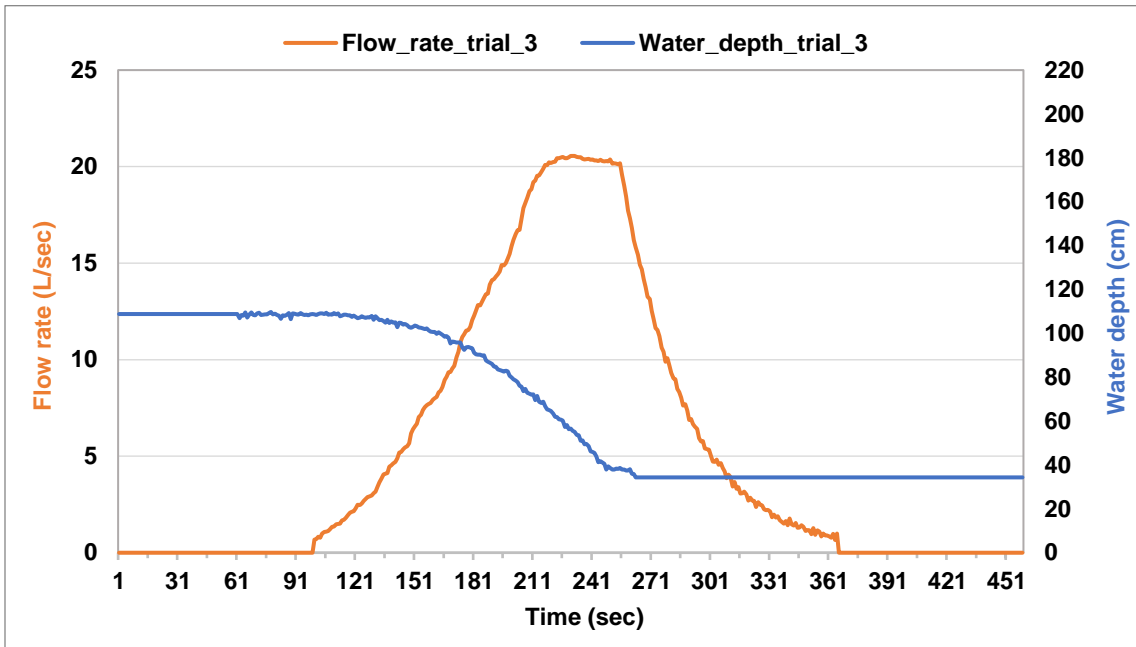
Figure 36. Result of Experiment 3 for controlled siphon system with 50% initial water depth (6-inch diameter actuated butterfly valve)
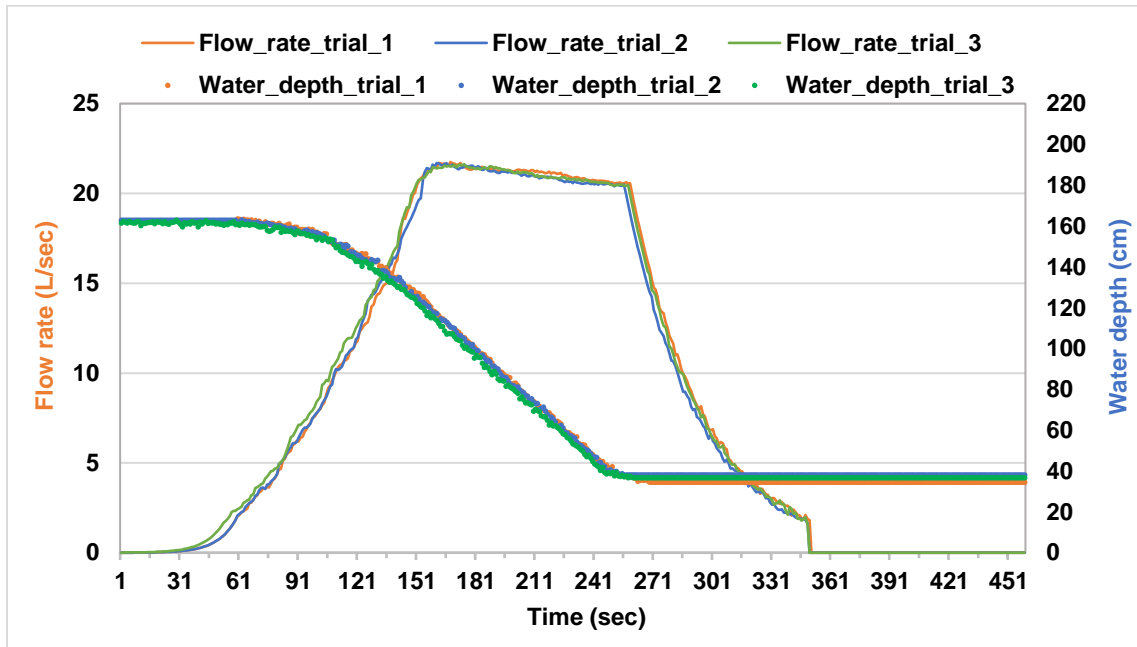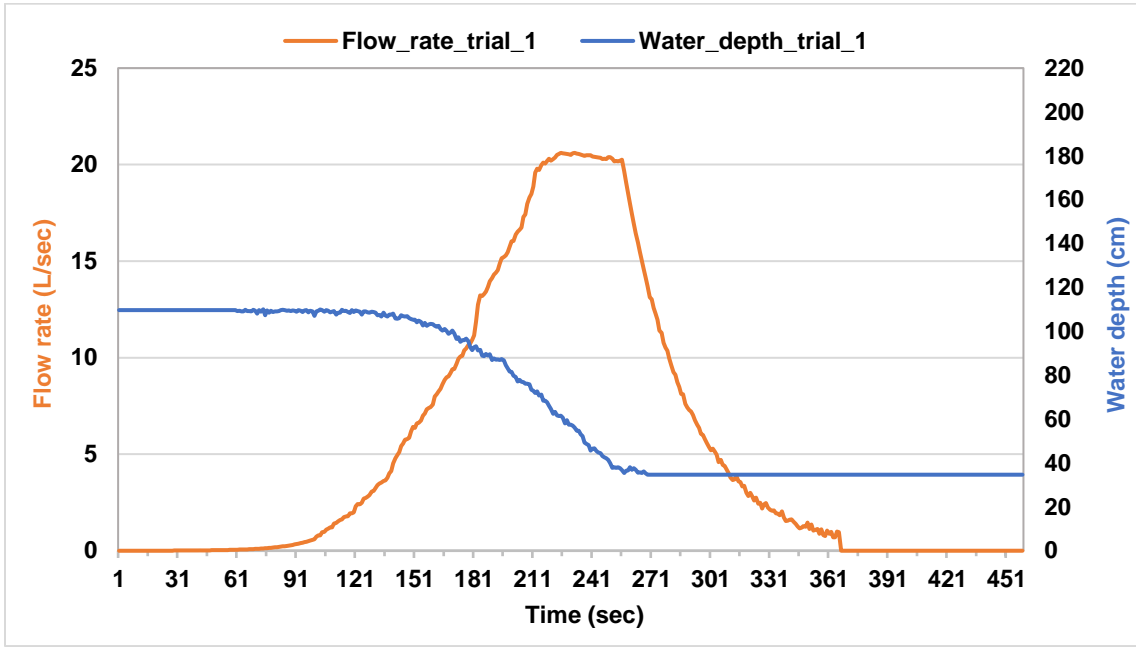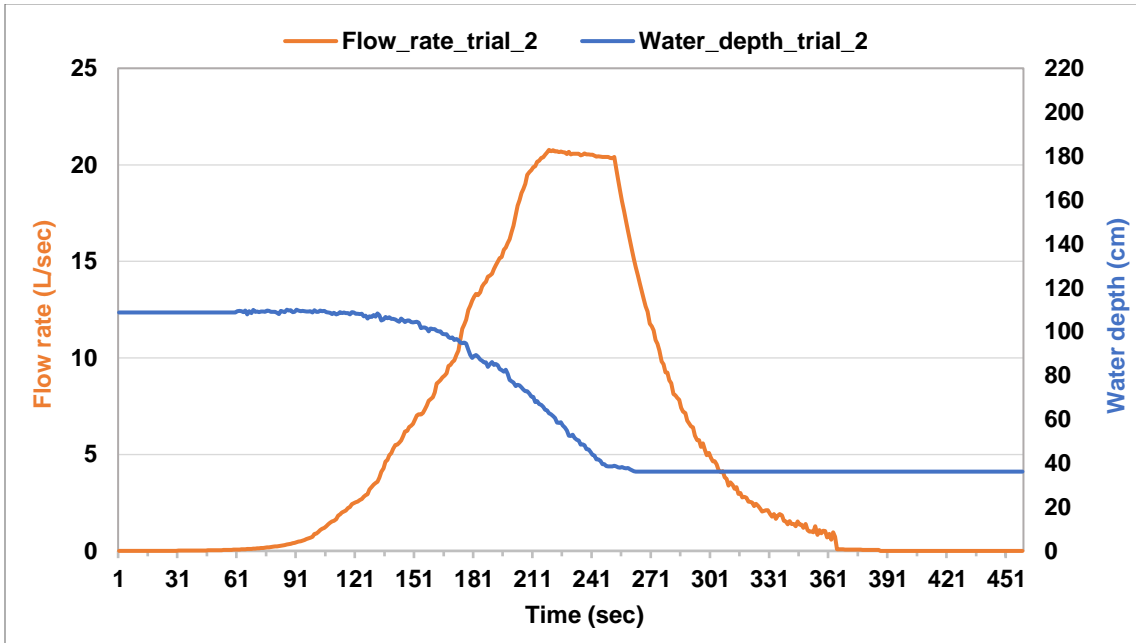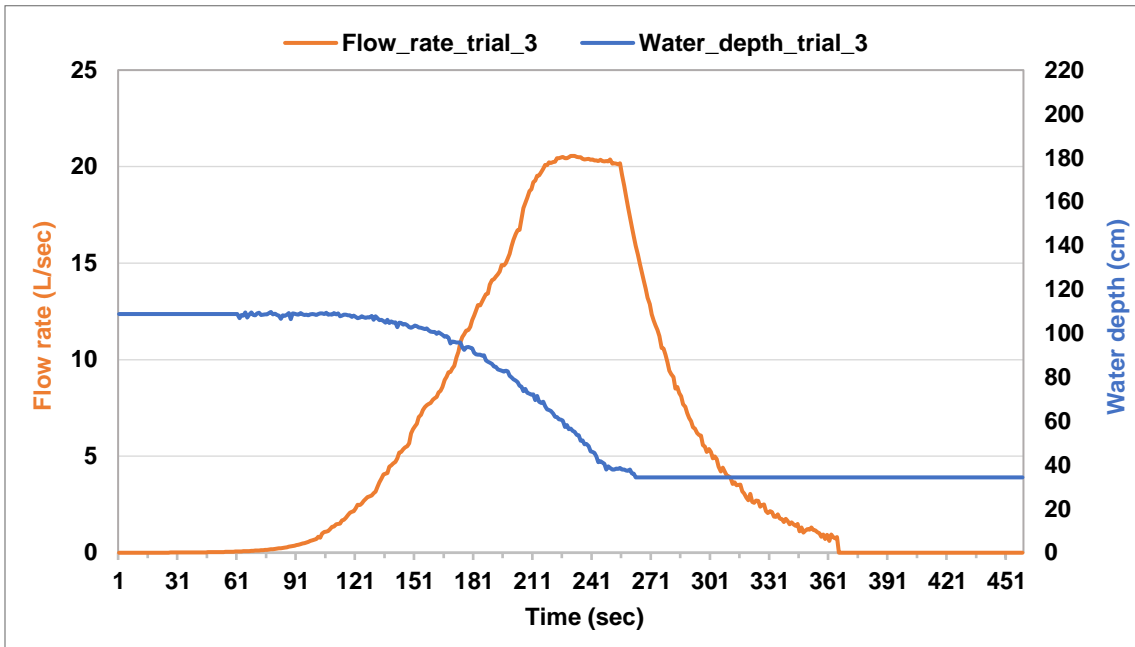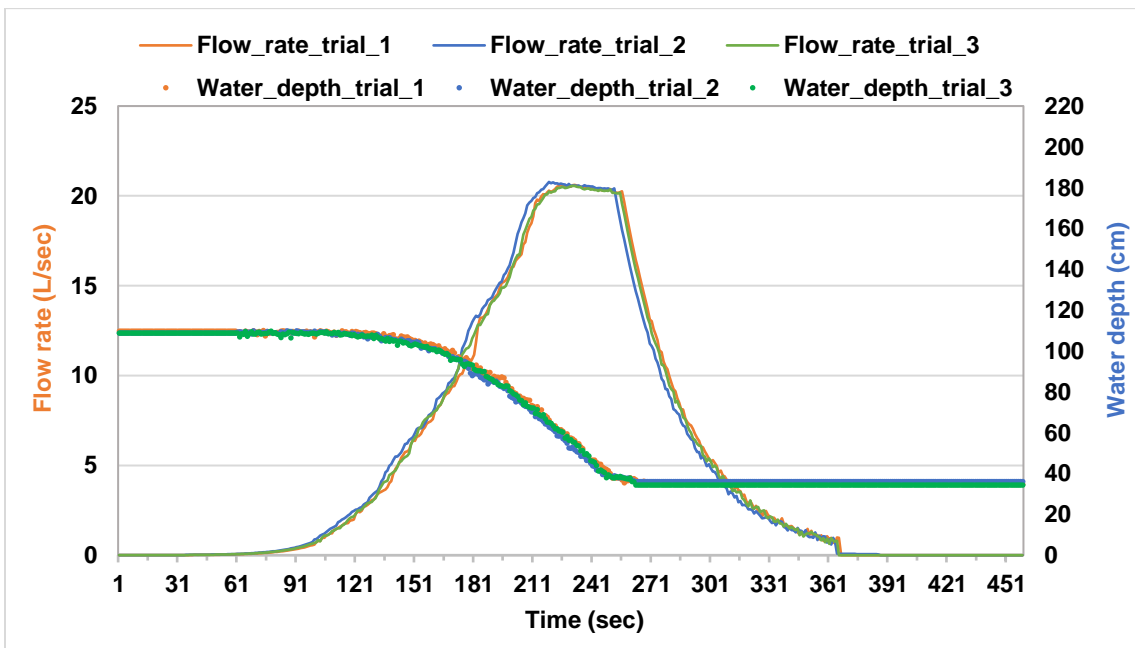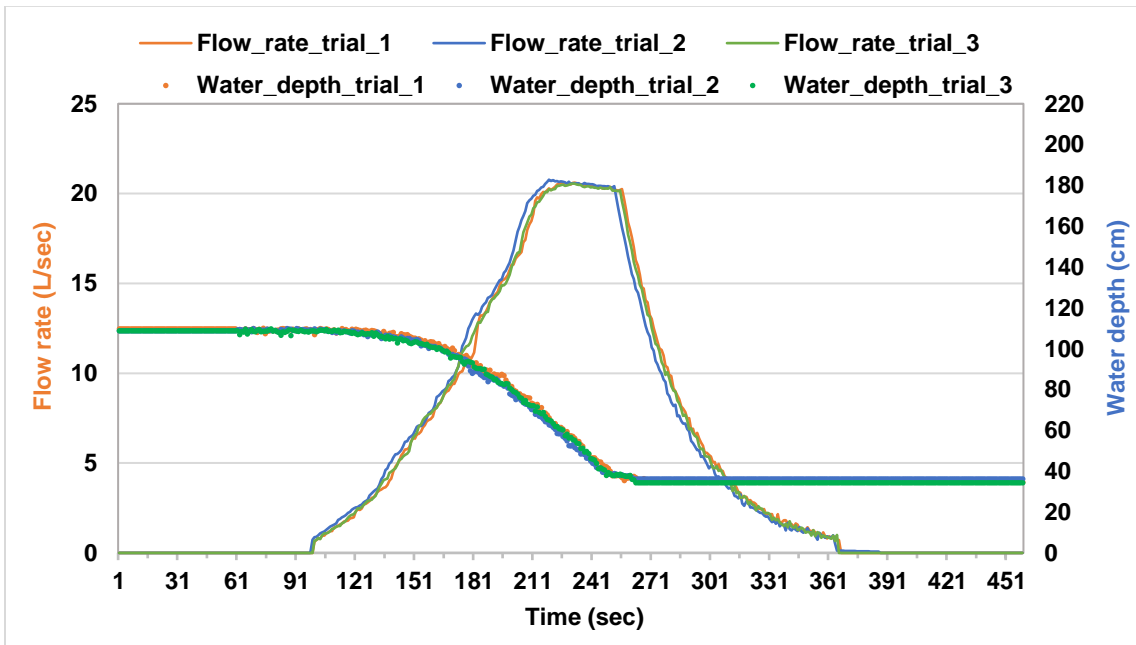

Figure 37. Result of Experiment 1, 2, and 3 for controlled siphon system with 50% initial water depth (6-inch diameter actuated butterfly valve)

The results from the above experiments performed at Florida Internal University (FIU) illustrate the siphon system's proper functioning under different initial water depth conditions. Every scenario is performed multiple times with two different types of conditions, slow and fast opening of an actuated butterfly valve. The results demonstrate the reproducibility of the experiments from the proposed siphon system.

The experimental results are then verified using statistical analysis such as sum, average, and variance. The results are illustrated in Tables 3, 4, and 5 for the slow opening of the actuated butterfly valve and Tables 6, 7, and 8 for fast opening of actuated butterfly valve for 50%, 75%, and 100% initial water depth, respectively.

Table 3. Flow release test for slow opening valve with 50% initial water depth

Groups	Count	Sum	Average	Variance
Trial 1	459	2447.97	5.33	48.91
Trial 2	459	2447.27	5.33	49.11
Trial 3	459	2439.94	5.32	48.50

Table 4.Flow release test for slow opening valve with 75% initial water depth

Groups	Count	Sum	Average	Variance
Trial 1	459	3871.04	8.43	74.60
Trial 2	459	3799.75	8.28	72.91
Trial 3	459	3903.37	8.50	73.94

Table 5. Flow release test for slow opening valve with 100% initial water depth

Groups	Count	Sum	Average	Variance
Trial 1	459	5156.61	11.23	84.91
Trial 2	459	5168.88	11.26	85.58
Trial 3	459	5172.58	11.27	85.41

Table 6. Flow release test for fast opening valve with 50% initial water depth

Groups	Count	Sum	Average	Variance
Trial 1	459	2438.58	5.31	49.12
Trial 2	459	2435.81	5.31	49.37
Trial 3	459	2429.23	5.29	48.74

Table 7. Flow release test for fast opening valve with 75% initial water depth

Groups	Count	Sum	Average	Variance
Trial 1	459	3852.88	8.39	75.23
Trial 2	459	3781.59	8.24	73.53
Trial 3	459	3888.31	8.47	74.47

Table 8. Flow release test for fast opening valve with 100% initial water depth

Groups	Count	Sum	Average	Variance
Trial 1	459	5134.57	11.19	85.93
Trial 2	459	5146.84	11.21	86.60
Trial 3	459	5150.55	11.22	86.43

All the statistical results for slow and fast opening actuated butterfly valve with different initial water depth conditions show that the sum, average, and the variance are very close to each other and hence can be statistically ensured that experiments are reproducible.

4.2 Analytical analysis and hydraulic performance of siphon system

The experimental results agree with the analytical verification that was reported for the siphon hydraulic system by Ozecik (2021); the same reference demonstrated that the results are replicated for the different pipe diameters in the siphon hydraulic system.

4.3 Operational reliability of the RBD Model for the siphon system

It is essential to use a reliable data source to perform an accurate analysis of operational reliability. If data is available from the facility or vendor, it is better to perform the analysis using these data. Unfortunately, most of the siphon component suppliers lack the required data. However, most of the suppliers provided information on life expectancy and warranty. Based on these two pieces of information, a reasonable assumption is proposed by taking references from the literature. Therefore, this study's primary purpose is to evaluate the operational reliability of the siphon system based on different system

architectures by assuming a failure probability for each of the components (Wang et al., 2004).

Furthermore, to make the TTF assumption for each component reasonable, the L_{10} life expectancy of each component is applied to estimate the scale parameter ($1/\lambda$). L_{10} life expectancy means the time at which 10% of a component will be broken (Carmody and Rea, 2014). Therefore, life expectancy can be expressed using equation 3 and 4 and is shown below

$$LEx = L_{10} = \frac{1}{\lambda}\left[-\ln\left[1 - P_f(L_{10} \le t)\right]^{\frac{1}{a}}\right] \tag{8}$$

Where P_f is the probability of failure.

Then λ is calculated from equation 8 and is expressed as below

$$\lambda_{LEx} = \frac{1}{LEx}(0.1054)^{\frac{1}{a}} \tag{9}$$

It is a general practice that the supplier lowers the failure probability of the selling product within the warranty period to minimize the warranty cost (Tian, 2006). Therefore, the warranty period can be calculated with the equation below,

$$T_w = \frac{1}{\lambda}\left[-\ln\left[1 - P_f(T_w \le t)\right]^{\frac{1}{a}}\right] \tag{10}$$

Then λ calculated from failure probability within warranty can be expressed as below

$$\lambda_{Pf} = \frac{1}{T_w}\left[-\ln\left[1 - P_f(T_w \le t)\right]^{\frac{1}{a}}\right] \tag{11}$$

Multiple experiments were performed with a total of hundred level switches (L.S.). Out of those hundred L.S., three were broken during the warranty period. Therefore, the failure probability is assumed to be 3% in this study. The scale parameter indicates the difference in failure classes (Carmody and Rea, 2014). The literature review suggests employing $a = 3.0$ for wear-out failures of the component (Carmody and Rea, 2014). Table 9 illustrates the input parameters for the model.

Table 9. The simulation parameters of each component of the siphon system

Component	LEx (year)	T_w (year)	$P_f(T_w<t)$	λ_{P_f}	λ_{LEx}	TTF a	λ	β
LS	-	2	.03	.1562	-	3	.1562	6.40
BP	5	3	-	-	.0945	3	.0945	10.59
AV	8	1	-	-	.0590	3	.0590	16.94
ABV	25	3	-	-	.0190	3	.0190	52.93
PLC	12	2	-	-	.0394	3	.0394	25.41
VPN	10	-	-	-	.0472	3	.0472	21.17

Based on the above data, the assumed PDF of TTF for all the components is shown in Fig. 38.
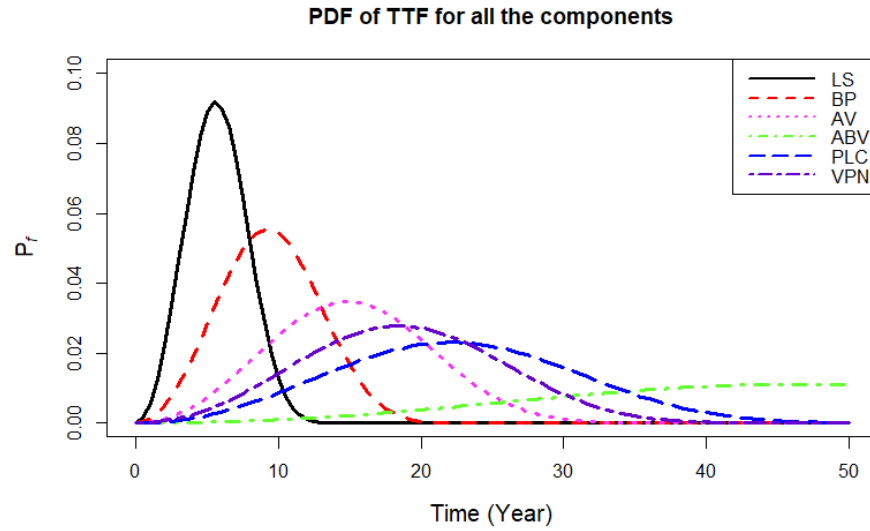
Figure 38. Weibull probability density distribution of TTF for all the components

Fig. 39 shows the simulation results for the system operational reliability with and without maintenance obtained from ExtendSim RBD for the four simulation scenarios (with a redundancy of 0, 1, 2, and 3). The siphon system's operational reliability with different maintenance times (2, 3, 4 years) are shown in Fig. 40, 41, and 42 and are computed using equation 5.
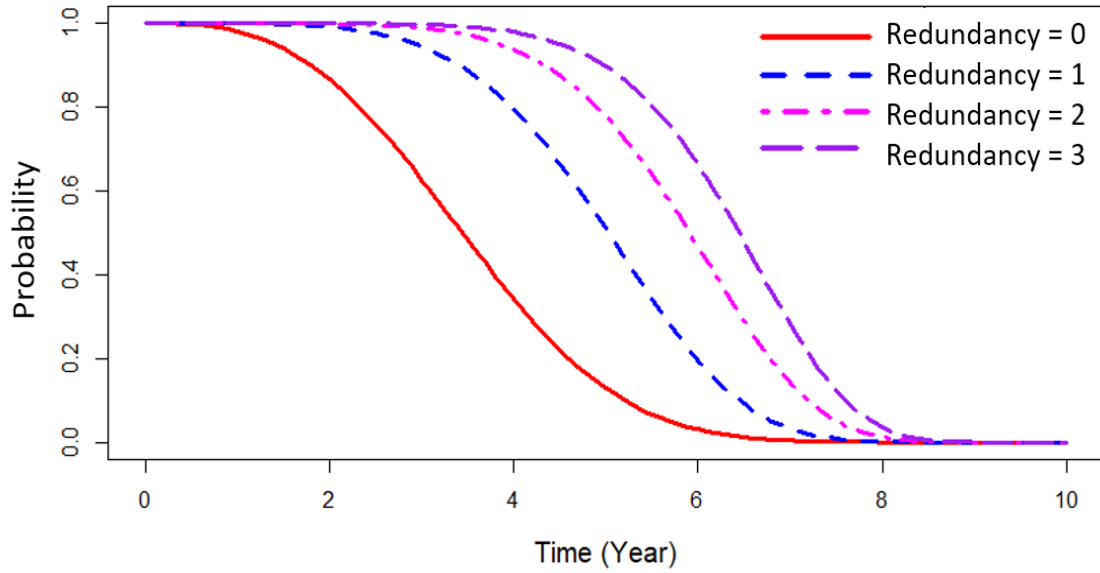
Figure 39. The siphon system's operational reliability for four scenarios with redundancy of 0, 1, 2, and 3

As shown in Fig. 39, the siphon system's operational reliability without redundancy (redundancy of 0) is about 0.20 around year five. The operational reliability increases with increasing redundancy, as shown in Fig. 40, 41, and 42, and it reaches about 0.90 for redundancy of 3 for the same period.
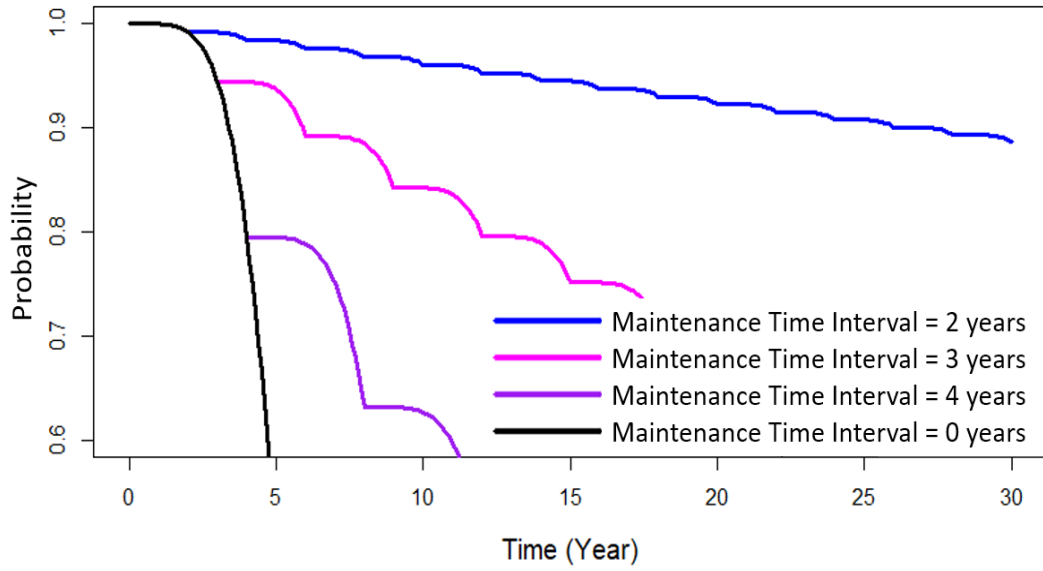
Figure 40. The operational reliability of the siphon system with a redundancy of 1 for four maintenance time intervals
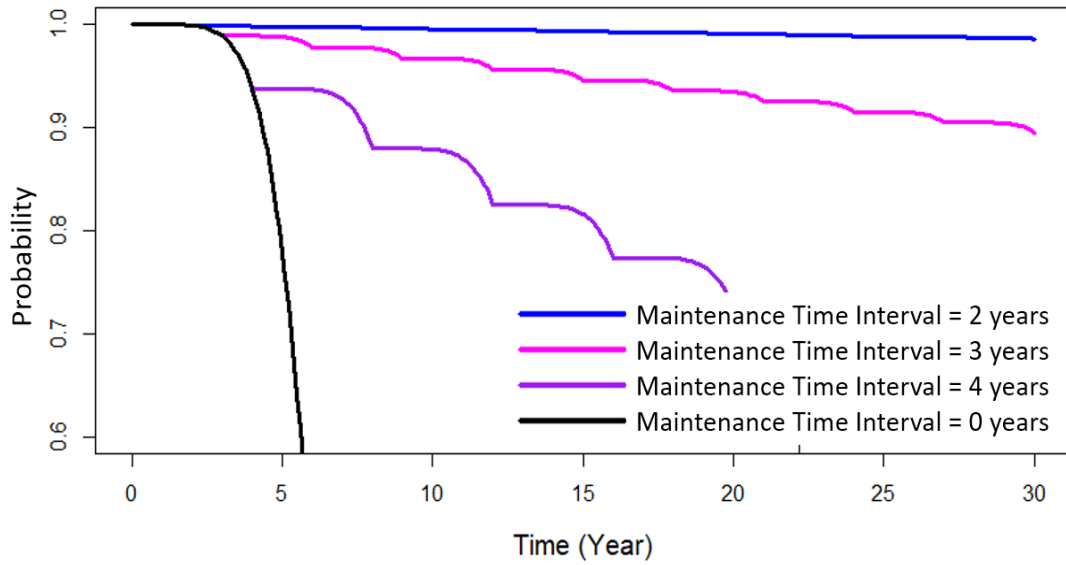
Figure 41. The operational reliability of the siphon system with a redundancy of 2 for four maintenance time intervals
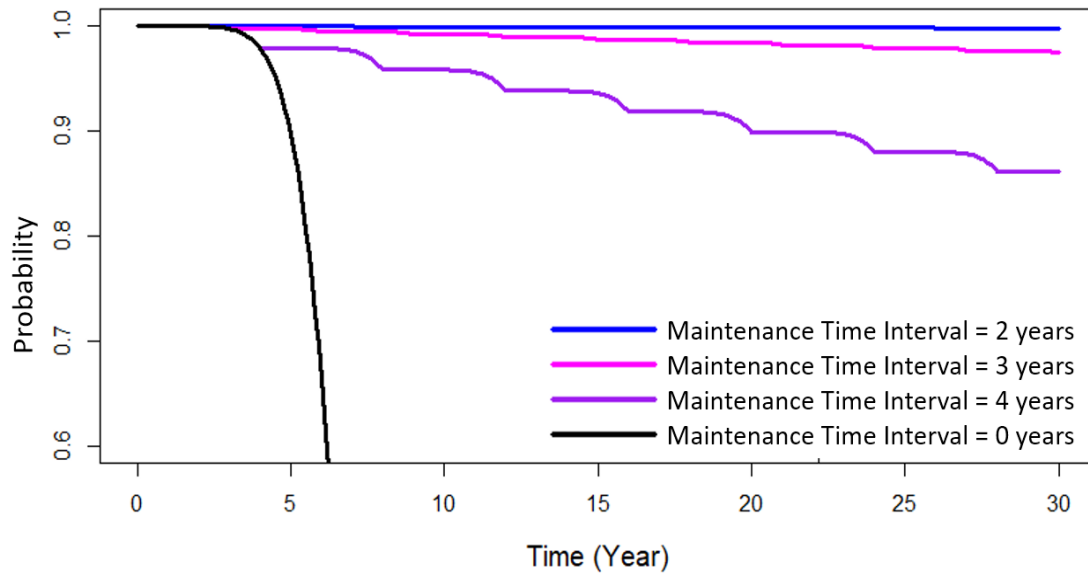
Figure 42. The operational reliability of the siphon system with a redundancy of 3 for four maintenance time intervals

The operational reliability can be increased with maintenance time. For instance, for a life expectancy of L_{10} (time at which 10% of a component will be broken) i.e., the siphon system's operational reliability should be above 0.90, and the designed life expectancy is over 20 years. Only three configurations meet the requirements – (a) siphon system with the redundancy of 1 for a period of maintenance of 2 years, (b) siphon system with the redundancy of 2 for a period of maintenance of 3 years, and (c) siphon system with the redundancy of 3 for a period of maintenance of 4 years.

4.4 Cost analysis of the siphon system consisting of three redundancies

Tables 10, 11, and 12 provide the installation cost of the siphon system if installed in the year 2020. Table 10 shows the installation cost of the siphon system consisting of three redundancies. Table 11 illustrates the maintenance cost analysis of nine scenarios consisting of three redundancies, three periods of maintenance (2, 3, and 4 years) for three

life spans (2020-39, 2020-49, 2020-69). Finally, Table 12 provides the total cost analysis by combining Table 10 and Table 11.

The first column, Tables 11 and 12, represents the redundancy and period of maintenance. For instance, Redundancy 1, 2 years means the system has a redundancy of one with two years of the maintenance period. The second column in Tables 10, 11, and 12 shows the cost of each aspect in 2020. The 3-5 columns of Tables 11 and 12 presents the cumulative cost of the setup, assuming that the system enters in service in 2020, and the periods of service are 20, 30, and 50 years, respectively. The average inflation rate of 2.165% is employed to compute the 3-5 columns of Tables 11 and 12, the average U.S. inflation rate between 2000 and 2019 (https://www.calculator.net/inflation-calculator).

Table 10. Installation cost of siphon system $2020 consisting of three redundancies

Installation Cost	Installation Cost $2020
Redundancy 1	$2,608.00
Redundancy 2	$2,732.00
Redundancy 3	$2,856.00

Table 11. Maintenance cost analysis of 9 scenarios consisting of three redundancies, three periods of maintenance and three life spans

Maintenance Cost	Maintenance cost $ 2020	Cumulative maintenance cost $ 2020-2039	Cumulative maintenance cost $ 2020-2049	Cumulative maintenance cost $ 2020-2069
Redundancy 1, 2 years	$ 1,166	$ 14,406.12	$ 22,846.22	$ 49,933.44
Redundancy 1, 3 years	$ 1,166	$ 8,813	$ 14,670.11	$ 33,644.18
Redundancy 1, 4 years	$ 1,166	$ 5,804.56	$ 11,667.74	$ 25,501.40
Redundancy 2, 2 years	$ 1,444	$ 16,198.86	$ 28,293.29	$ 61,838.67
Redundancy 2, 3 years	$ 1,444	$ 10,914.47	$ 18,167.80	$ 41,665.68
Redundancy 2, 4 years	$ 1,444	$ 7,188.52	$ 14,449.61	$ 31,581.50
Redundancy 3, 2 years	$ 1,736	$ 19,474.52	$ 34,014.63	$ 74,343.46
Redundancy 3, 3 years	$ 1,736	$ 13,121.55	$ 21,841.61	$ 50,006.34
Redundancy 3, 4 years	$ 1,736	$ 8,642.14	$ 17,371.54	$ 37,967.79

Table 12. Total cost analysis of 9 scenarios consisting of installation cost $2020 with three redundancies, three periods of maintenance and three life spans

Total Cost	Reliab ility	Installation Cost $ 2020	Cumulative cost $ 2020-2039	Cumulative cost $ 2020-2049	Cumulative cost $ 2020-2069
Installation cost + redundancy 1, 2 years	0.94	$ 2,608.00	$ 17,014.12	$ 25,454.22	$ 52,541.44
Installation cost + redundancy 1, 3 years	0.84	$2,608.00	$ 11,421.20	$ 17,278.11	$ 36,252.18
Installation cost + redundancy 1, 4 years	0.63	$2,608.00	$ 8,412.56	$ 14,275.74	$ 28,109.40
Installation cost + redundancy 2, 2 years	0.98	$2,732.00	$ 18,930.86	$ 31,025.29	$ 64,570.67
Installation cost + redundancy 2, 3 years	0.96	$2,732.00	$ 13,646.47	$ 20,899.80	$ 44,397.68
Installation cost + redundancy 2, 2 years	0.89	$2,732.00	$ 9,920.52	$ 17,181.61	$ 34,313.50
Installation cost + redundancy 3, 2 years	0.99	$2,856.00	$ 22,330.52	$ 36,870.63	$ 77,199.46
Installation cost + redundancy 3, 3 years	0.98	$2,856.00	$ 15,977.55	$ 24,697.61	$ 52,862.34
Installation cost + redundancy 3, 4 years	0.96	$2,856.00	$ 11,498.14	$ 20,227.54	$ 40,823.79

Industrial decision-makers using engineering economic analysis are concerned with magnitude and timing of a project's cash flow and total profitability of that project. In this situation, a method is required to compare projects involving receipts and disbursements

occurring at different times. The equivalence of any future amount to any present amount

is called present value, tabulated in Table 13, and computed from equation 12.

$$\text{Present Value} = \frac{FV}{(1+r)^n} \qquad (12)$$

Where FV = Future Value, r = rate of interest, n = no. of years

Table 13. Present value of the total cost analysis of 9 scenarios consisting of installation
cost $2020 with three redundancies, three periods of maintenance and three life spans

Total Cost	Installation Cost $ 2020	Cumulative cost $ 2020-2039	Cumulative cost $ 2020-2049	Cumulative cost $ 2020-2069
Installation cost + redundancy 1, 2 years	$ 2,608	$ 11,873	$ 15,431	$ 28,157
Installation cost + redundancy 1, 3 years	$2,608	$ 7,970	$ 10,475	$ 19,428
Installation cost + redundancy 1, 4 years	$2,608	$ 5,870	$ 8,654	$ 15,604
Installation cost + redundancy 2, 2 years	$2,732	$ 13,210	$ 18,809	$ 34,603
Installation cost + redundancy 2, 3 years	$2,732	$ 9,523	$ 12,770	$ 23,793
Installation cost + redundancy 2, 2 years	$2,732	$ 6,922	$ 10,416	$ 18,388
Installation cost + redundancy 3, 2 years	$2,856	$ 15,583	$ 22,352	$ 41,371
Installation cost + redundancy 3, 3 years	$2,856	$ 11,149	$ 14,971	$ 28,329
Installation cost + redundancy 3, 4 years	$2,856	$ 8,024	$ 12,262	$ 21,877

CHAPTER 5: CONCLUSIONS AND RECOMMENDATIONS

5.1 Conclusions

This dissertation presents a low-cost and reliable integrated hardware and software architecture for remote water release. The two integrated systems are presented to release water from storage units (ponds, reservoirs, and wetlands) using the siphon hydraulic system. One of the systems is based on Antenna and Software Defined Radio (SDR) technology, and another one is based on Internet of Things (IoT) technology. Both the systems provide local and global communication; however, the remote update is possible only in IoT based technology.

Both the systems use the hardware components such as water level sensors, air vent, bilge pump, and actuated butterfly ball valve. The hardware components are installed in the field that collects the data and transmits it to the remote center via a Programmable logic controller (PLC). The data is analyzed in the remote center and returned with the operations needed to be performed in the field. The systems established two-way communication, and hence the data is collected, transferred, and analyzed. The remote operation is performed using 4G/5G cellular connection.

A new software interface in C# language is designed and developed to control and monitor gate operations for the siphon hydraulic system and summarize the near real-time status of devices employed in the field. The gate operations can be performed manually and/or automatically. The interface can also be used to check the functioning or malfunctioning of the devices.

An entire experimental facility is developed to demonstrate the applicability of the proposed systems. A series of laboratory testing, collecting data, and its analysis were performed at FIU. The lab setup includes multiple 6-inch diameter siphon and conventional drainage pipe systems. The total length of the siphon pipe and conventional drainage pipe is approximately 25 feet and 15 feet, respectively. The capacity of the tank is 2,500 gallons with 90-inch in diameter and 98-inch in height. The flow discharge data has been acquired using the Omega FDT-40 transit time ultrasonic flow meter; meanwhile, the water level has been measured using Omega LVCN 414. Both instruments are connected to the NI-6323 data acquisition instrument through the SCB-64A terminal.

The experimental results indicate that the systems are reliable. Reliability is defined as the probability that the system will perform its intended function adequately without failure. The operational reliability of hardware components such as liquid level sensors, bilge pumps, and air vents has been analyzed using the Reliability Block Diagram (RBD) in the ExtendSim platform. The results of the operational reliability of the system are obtained through Monte Carlo simulations.

The cost analysis of the proposed systems has also been performed. The cost analysis includes the installation cost, maintenance cost, and the total cost of the proposed systems. It also provides redundancy and components' life span. Several scenarios were analyzed that consist of three redundancies (1, 2, and 3) and three periods of maintenance (2, 3, and 4 years) for three life spans (2020-39, 2020-49, 2020-69). The average inflation rate of

2.165%, the average U.S. inflation rate between 2000 and 2019, is employed to compute life spans.

This research also provided an opportunity and comprehensive appendices to implement and develop integrated hardware and software platforms for researchers and users.

The new methodology for remote management of water storage units utilizing the hardware and software platform developed in this research proved to be capable of managing hundreds and even thousands of storage units effectively and economically. Also, laboratory testing showed that the platform is capable of implementing the management plans and schedule maintenance activities.

The key findings include:

(1) The proposed integrated hardware and software frameworks can be used to release water remotely from storage units and be applied to other purposes, such as mitigating floods, managing water levels in wetlands for ecological purposes.

(2) This study successfully implemented the work tested with a siphon hydraulic system and can also be readily implemented effectively in the conventional drainage pipe hydraulic system.

(3) The operational reliability of the siphon hydraulic system is directly proportional to the redundancy and period of maintenance. Therefore, the greater the redundancy and/or period of maintenance, the greater is the reliability.

(4) The cost analysis shows that the siphon hydraulic system with the communications network is approximately seven times cheaper than the currently employed SCADA system.

5.2 Recommendations

(1) The proposed system can be trained using Artificial Intelligence and Machine Learning to add another layer of reliability.

(2) Cybersecurity can be enhanced to secure technologies, devices, and processes.

(3) A mobile application can be made to monitor and operate the entire process.

(4) The users who want to implement the siphon hydraulic system to release water from storage units are highly recommended to follow the steps as provided in the appendices.

APPENDIX

APPENDIX A – Tutorial on PLC

Communication can be established between the PC and CPU when they are on the same network. The configuration for the PC and CPU to be in the same network is explained below-

PC Setup

The PC can be configured as outlined below:

1. Enter ncpa.cpl in the Run window.

2. Right-click on the Local Area Connection and select Internet Protocol (TCP/IP).

3. Enter the following - IP address: 192.169.1.2 and subnet mask: 255.255.255.0 and then select ok.

CPU Setup

The CPU can be configured as described below:

1. From the Productivity Suite Software, select CPU.

2. Select change CPU IP/Name option.

4. Enter the following - IP address: 192.169.1.2 and subnet mask: 255.255.0.0 and then select ok.

APPENDIX B – Tutorial on C# Interface

Step1: Double click on the provided exe file. Software interface will pop up as shown in

Fig. A-1.

Figure A-1. Main Software Interface for Siphon System

Step 2: Click "File" and then click "New" as shown in Fig. A-2, a storage editor will

pop-up as shown in Fig. A-3.
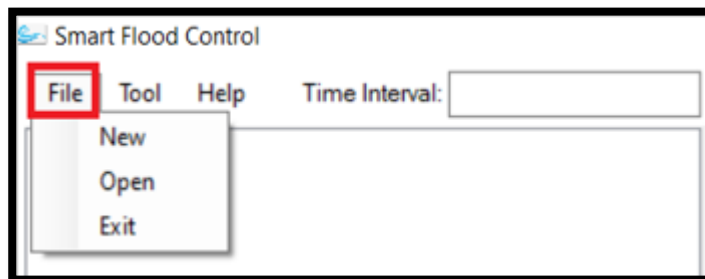
Figure A-2. Smart Flood Control Interface
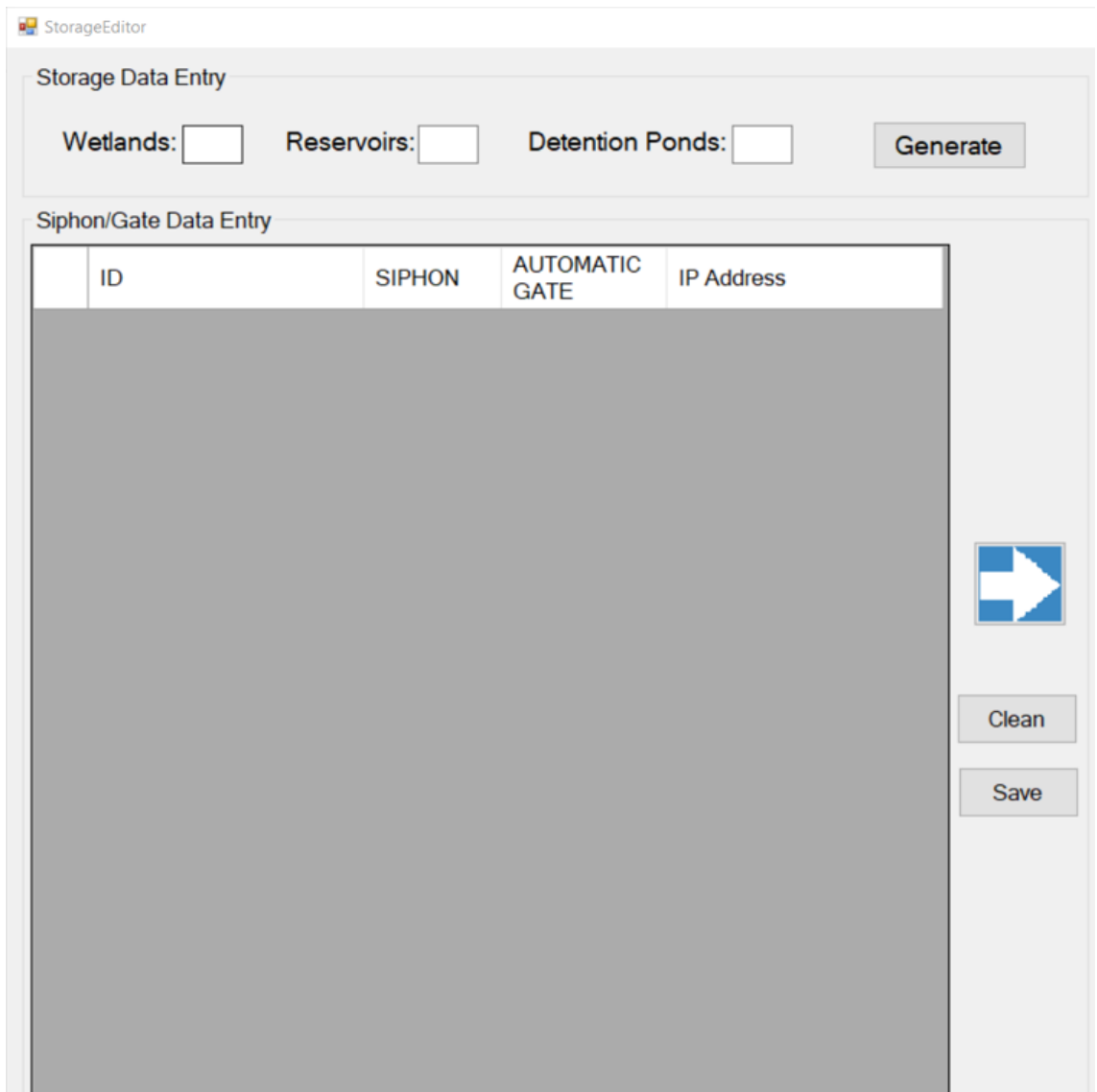
Figure A-3. Storage Editor

Step 3: Enter required number of wetlands, reservoirs, and ponds. Then, click "Generate" as shown in Fig. A-4.

Figure A-4. Storage Data Entry

Step 4: Input numbers of siphons and/or automatic gate and assign IP Address for each

storage units as shown in Fig. A-5 and Fig. A-6.

Figure A-5. Siphon/Gate Data Entry

Figure A-6. Enter numbers of siphon/automatic gates with IP Addresses

Step 5: Click blue arrow to generate the inputs entered by the user as shown in Fig. A-7.
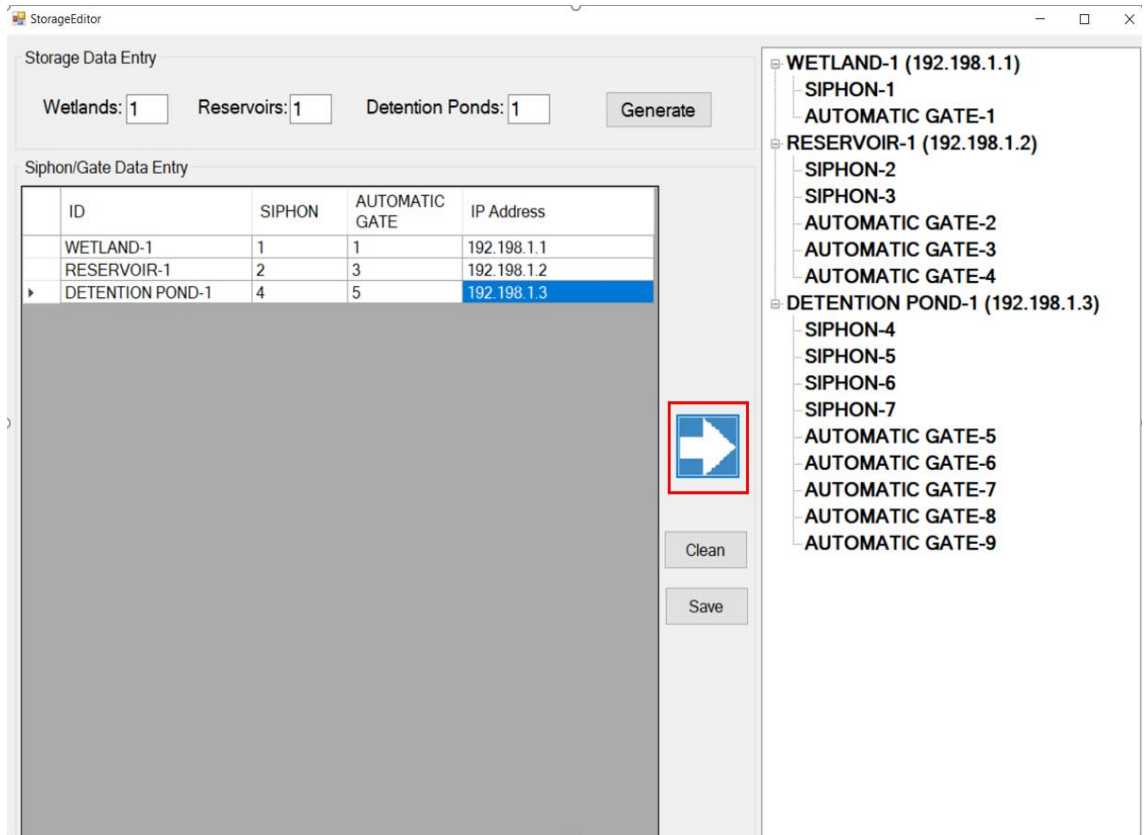
Figure A-7. Final input entered by the user

Step 6: Click "Save" the data of storage entry as shown in Fig. A-8.
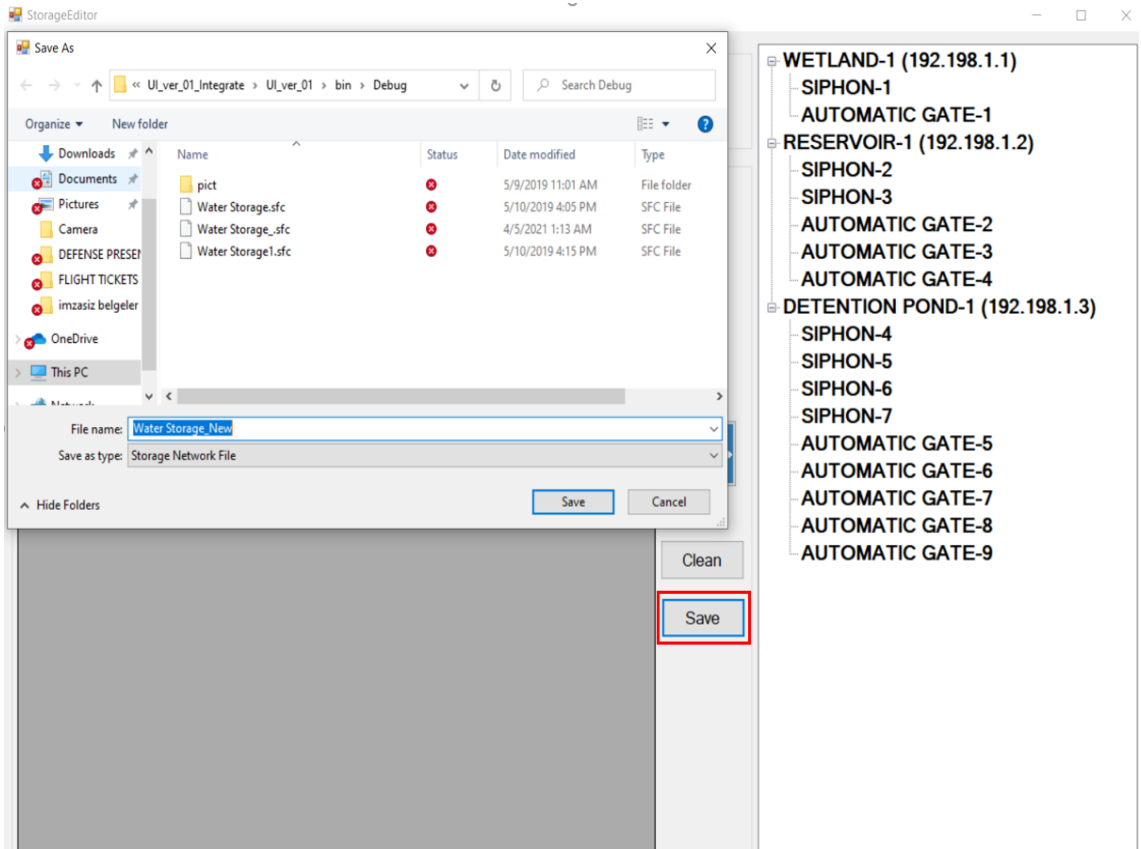
Figure A-8. Save Storage Entry Data

Step 7: Once the file is saved close the current tab. Then, from the "File" drop down menu select "Open" as shown in Fig. A-9 and choose the location where that file is saved as shown in Fig. A-10.
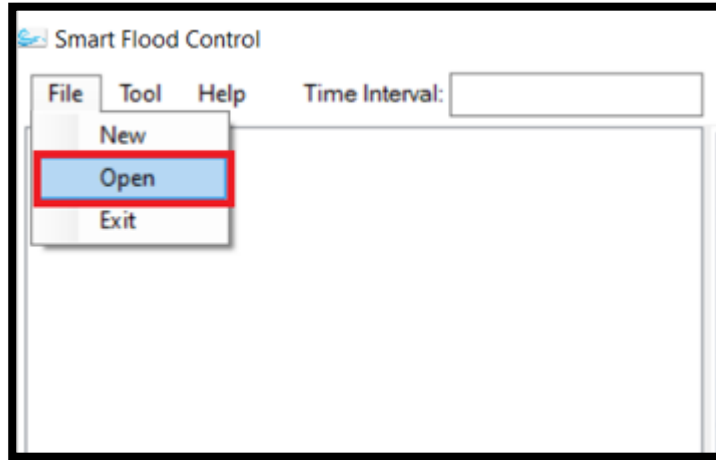
Figure A-9. Open saved file
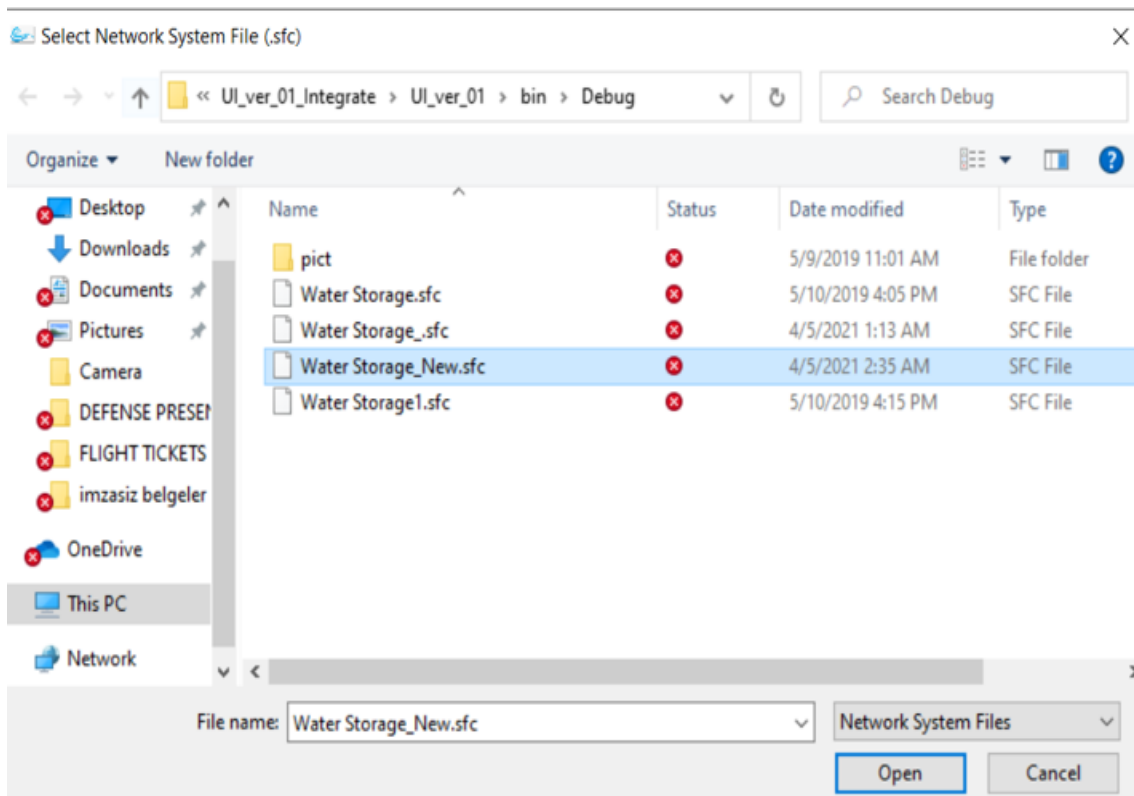
Figure A-10. Saved File location

Step 8: Once this process is done, the software interface will look as shown in Fig. A-11.
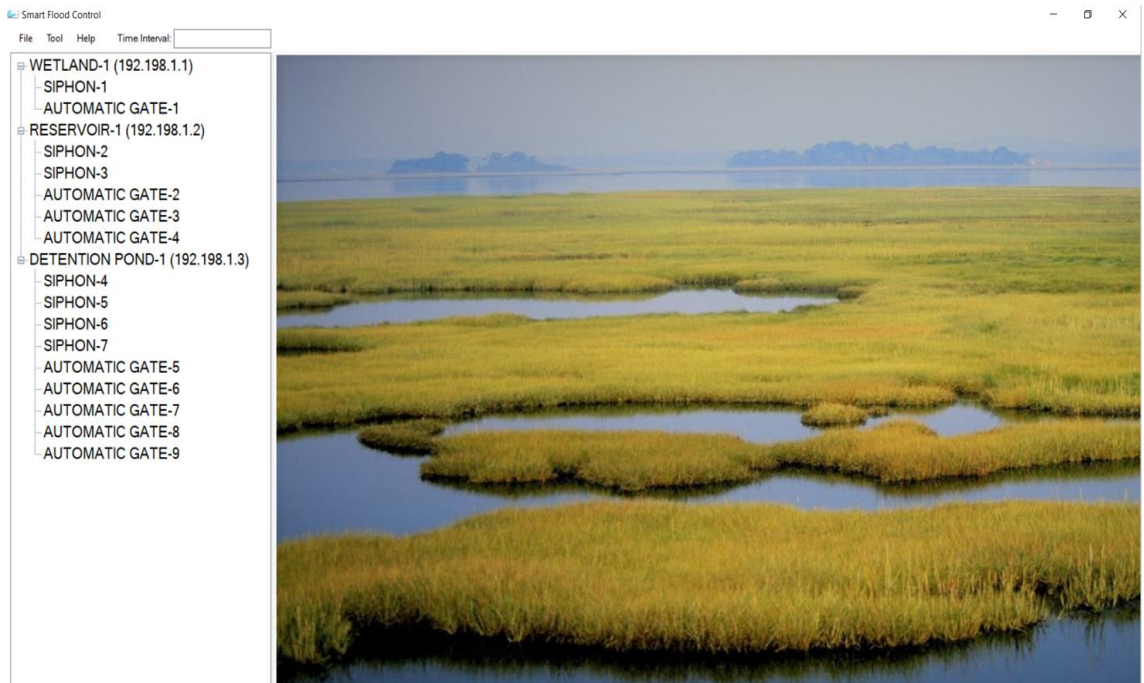
Figure A-11. Software interface after data entry generation

Step 9: Go to "Tool" menu option and click "Run" as shown in Fig. A-12. The software

interface will start working.
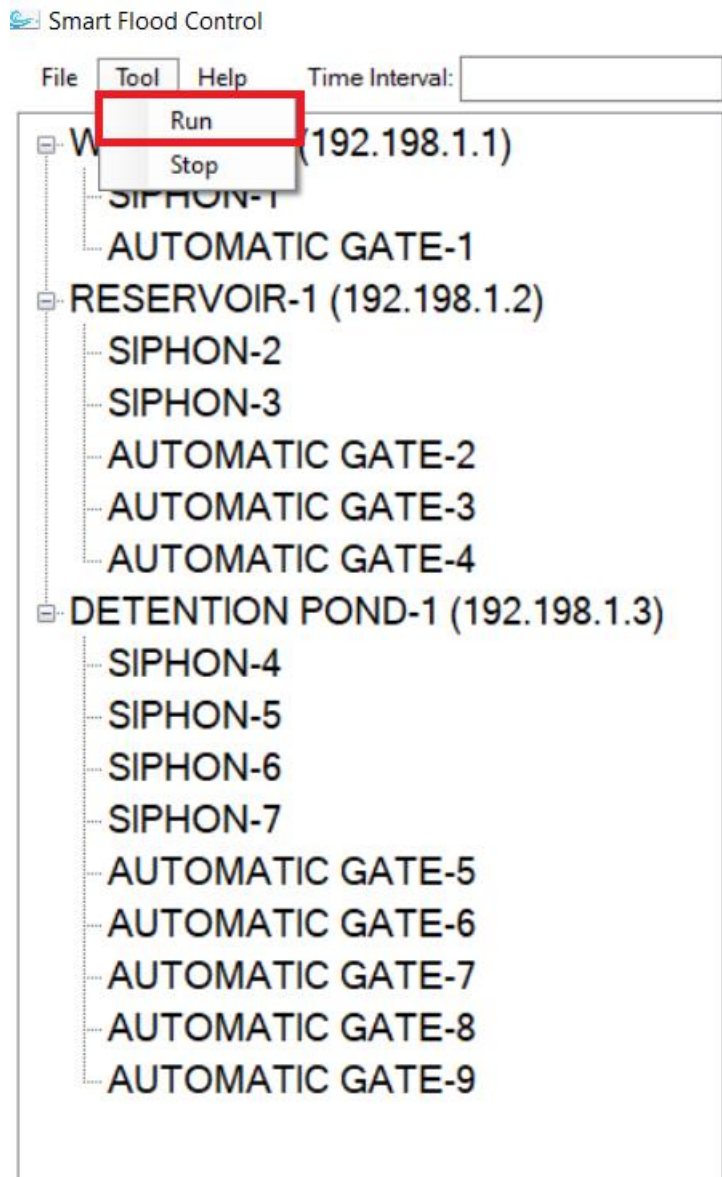
Figure A-12. Software interface will start working after "Run" is selected

APPENDIX C – Pseudo code

```
// storage system includes wetlands, ponds and reservoirs

for (int i = 0; i < the number of storage system; i++)

        {

           if (storage system [i] is provided)

          {

                Collect status of two Level switches in storage system [i];

              storage system [i]. Font = black;

                for (int j = 0; j < the number of siphons; j++)

             {

                if (siphon[j] is provided)

                {

                   siphon[j]. Font = Black;

                   Collect status of two Level Switches in siphon[j];

                if (water level in storage system > lower level switch in storage system [i])

                   {

                      if (water level in storage system > upper level switch in storage

system [i])

                         {

                            if (outlet gate is not opened)

                              {
```

```
                    if (water level in clear pipe > upper level switch in

siphon[j])

                        {

                          if (pump and air vent in siphon[j] are closed)

                            {

                                Open the outlet gate in siphon[j];

                            }

                          else turn off pump and close air vent in siphon[j];

                        }

                    else if (water level in clear pipe > lower level switch in

siphon[j])

                        {

                          if (pump and air vent in siphon[j] are closed)

                            {

                                Open the outlet gate in siphon[j];

                            }

                          }

                          else turn on pump and open the air vent in siphon[j];

                    }

                else if (received the order for opening the outlet gate)

                    {

                      if (outlet gate is not opened)

                        {
```

```
                    if (water level in clear pipe > upper level switch in
siphon[j])
                              {
                           if (pump and air vent in siphon[j] are closed)
                              {
                                Open the outlet gate in siphon[j];
                              }
                           else turn off pump and close air vent in siphon[j];
                              }
                        else if (water level in clear pipe > lower level switch in
siphon[j])
                              {
                           if (pump and air vent in siphon[j] are closed)
                              {
                                Open the outlet gate in siphon[j];
                              }
                              }
                        else turn on pump and open the air vent in siphon[j];
                         }
                      }
                  else
                   Close the outlet gate in siphon [j];
                   }
```

```
                else

                    turn off the pump, close air vent and outlet gate in siphon[j];

            }

        }

    for (int k = 0; k < the number of controlled gates; k++)

        {

            if (controlled gate[k] is provided)

            {

                controlled gate [k]. Font=Black;

                if (water level in storage system > lower level switch in storage system

[i])

                {

                    if (water level in storage system > upper level switch in storage

system [i])

                    {

                        Open the controlled gate [k];

                    }

                    else if (received the order for opening controlled gate [k])

                      {

                        Open controlled gate [k];

                      }

                     else

                         Close controlled gate [k];
```

```
        }

    else

        Close controlled gate[k];

    }

}

}

}
```

APPENDIX D – Experimental Results

A planar monopole antenna was designed for WiFi and Bluetooth frequencies on FR-4 material. The material was then fabricated using an LPKF laser. The signal is quickly attenuated in the planar monopole antenna at 2-5 GHz frequency. The Frii's is then used to compute the optimistic attenuation level for a chosen frequency, i.e., the equation is used to determine the distance in which a communication system can successfully transmit a signal.

$$P_r = \frac{P_t G_t G_r c^2}{(4\pi R f)^2} \tag{1}$$

Where P_r and P_t is the power received and transmitted respectively, G_t and G_r is the gain associated with the transmitting and receiving antenna, respectively, c is the speed of light, R is the distance between the two antennas, and f is the frequency of operation.

Fig. B-1 shows the conceptual understanding for the test performed in three parts to compute short and long-range transmission for the planar monopole antenna and the SDR. The left side of part 1 consists of a planar monopole antenna and the SDR; similarly, the right part also consists of another planar monopole antenna and the SDR. There is a certain distance (R_1) between the two. The result is obtained in the desired spectrum, and hence communication can be established among the two.

In the second part, the distance ($R_{2 > R_1}$) is increased between the two systems, and again the result is measured. In this case, the strength of the signal drops, and hence there may be some issues during communication. This problem can be solved in a couple of ways – either decrease the distance between the two systems or employ a more powerful antenna.

As distance cannot be reduced after a certain level, a more sustainable solution is to use a powerful antenna. So in part three, Horn antennas were used instead of one planar antenna to get back the desired spectrum.
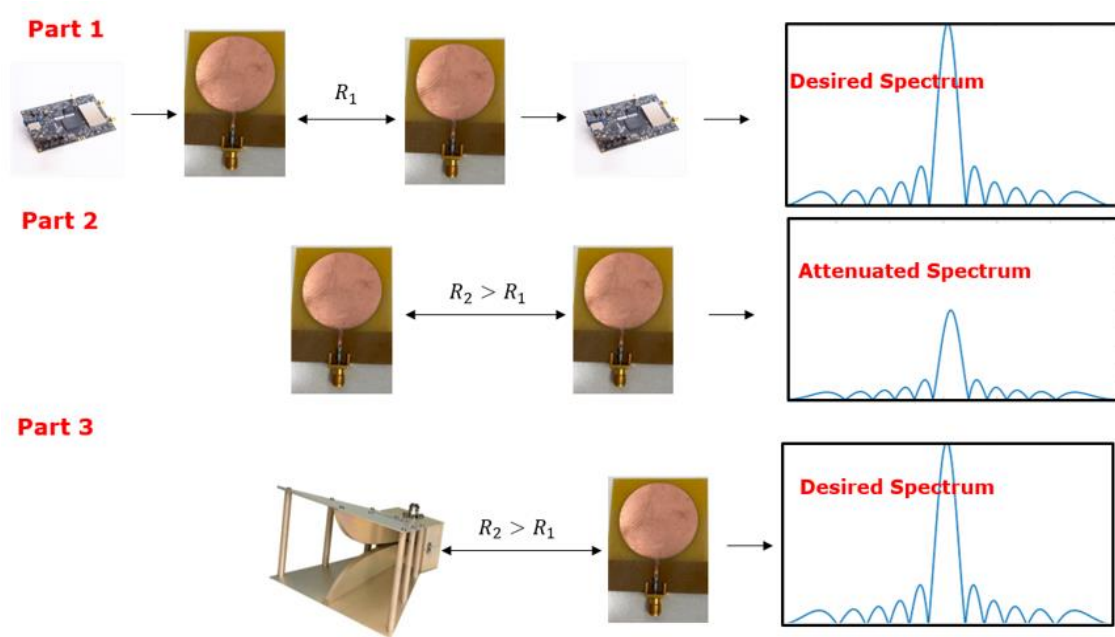
Figure B-1. Three-part experiments performed at RFCOM lab at FIU

Fig. B-2, B-3, and B-4 illustrated the results of three experiments performed at RFCOM lab at FIU, as shown above in Fig. B-1.

The first experiment is set up for 2 m transmission between the two sets (Receiver (Rx) and Transmission (Tx)) of SDR and planar monopole antenna as shown in Fig. B-2. The transmission results were analyzed using a spectrum analyzer and illustrated on the right side Fig. 39. For a given power of -5dBW at 2.4 GHz, SDR and antenna gains were 10 dB and 4 dB, respectively. For this setup, the signal power received was at -50dBW.

Figure B-2. Experimental setup for 2 meter transmission

For the second experiment, as shown in Fig. B-3, the distance is increased from 2 m to 10 m. The same procedure is followed as explained above for the first experiment. The signal power received is -62 dBW, i.e., it is dropped by 12 dBW from -50 dBW to -62 dBW. This setup is only applicable for short-range communication because the power is dropped by more than x100 with an x10 increase in distance.
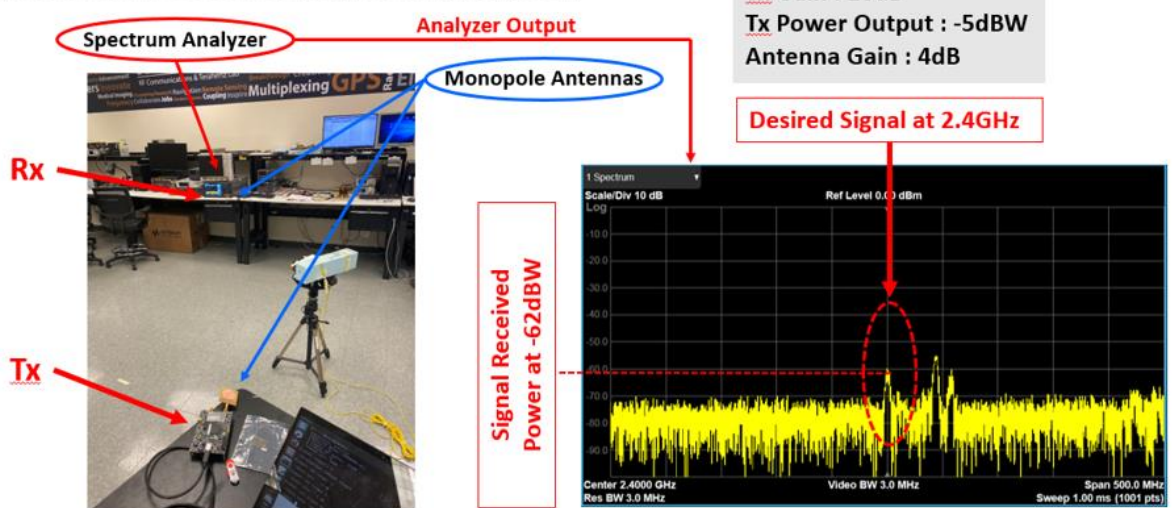
Figure B-3. Experimental setup for 10 meter transmission

The third experiment is shown in Fig. B-4 and is performed for the same distance as in the

second experiment i.e., for 10 m. However, one of the planar monopole antenna is replaced

with the more powerful Horn antenna, which gains 10 dB i.e., an additional 6 dB compared

with the planar monopole antenna. The signal power is received at -57 dBW, and thus by

implementing a horn antenna that has more gain, approximately 5 dB gain is increased.
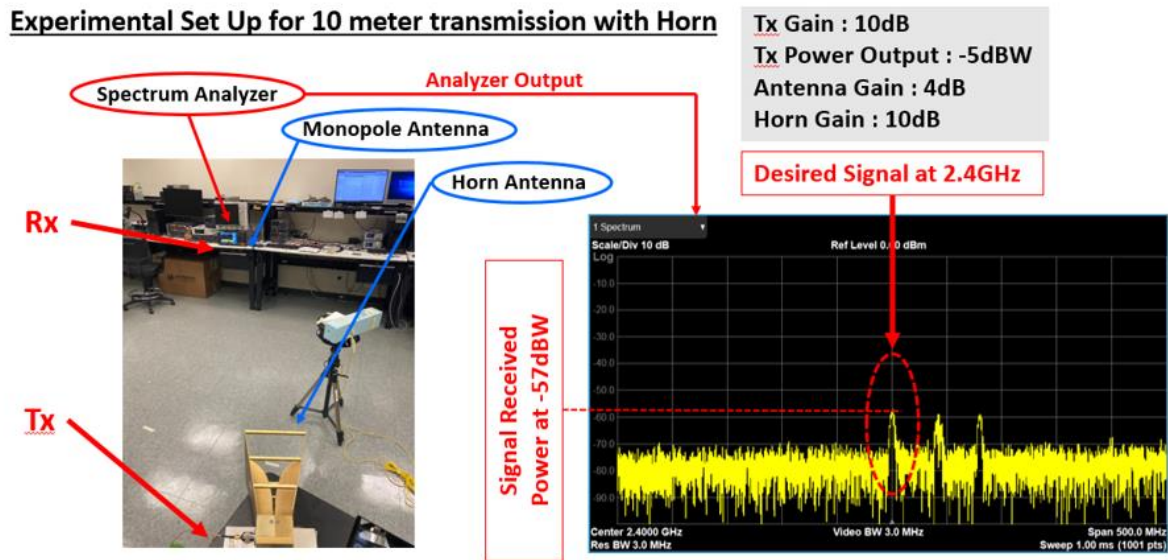
Figure B-4. Experimental setup for 10 meter transmission with Horn

The proposed system is suitable for short-range communication at 2.4 GHz. The long range

communication can be achieved using lower frequencies such as 700 MHz.

REFERENCES

Abbasi, S., 2002. Water quality indices state-of-the-art. Pondicherry: Pondicherry University, Centre for Pollution Control & Energy Technology.

Abdelkarim, A., Gaber, A.F., Youssef, A.M., Pradhan, B., 2019. Flood Hazard assessment of the Urban area of Tabuk City, Kingdom of Saudi Arabia by integrating spatial-based hydrologic and hydrodynamic modeling. Sensors 19(5), 1024.

Azman, A.A., Rahiman, M.H.F., Taib, M.N., Sidek, N.H., Bakar, I.A.A., Ali, M.F., 2016. A low cost nephelometric turbidity sensor for continual domestic water quality monitoring system, 2016 IEEE International Conference on Automatic Control and Intelligent Systems (I2CACIS). IEEE, pp. 202-207.

Bekele, E.G., Nicklow, J.W., 2007. Multi-objective automatic calibration of SWAT using NSGA-II. Journal of Hydrology 341(3-4), 165-176.

Bian, L., Verma, V., Rojiali, A., Zanje, S.R., Ozecik, D., Leon, A.S., 2020. Operational Reliability Assessment of a Remotely-controlled Siphon System for Draining Shallow Storage Ponds.

Bordalo, A.A., Teixeira, R., Wiebe, W.J., 2006. A water quality index applied to an international shared river basin: the case of the Douro River. Environmental management 38(6), 910-920.

Breckpot, M., Blanco, T.B., De Moor, B., 2010. Flood control of rivers with nonlinear model predictive control and moving horizon estimation, 49th IEEE conference on decision and control (CDC). IEEE, pp. 6107-6112.

Brown, R.M., McClelland, N.I., Deininger, R.A., Tozer, R.G., 1970. A water quality index-do we dare. Water and sewage works 117(10).

Bullock, A., Acreman, M., 2003. The role of wetlands in the hydrological cycle. Hydrology and Earth System Sciences 7(3), 358-389.

Carmody, C., Rea, C., 2014. Predicting product life expectancy of the LabTecta bearing protector. Sealing Technology 2014(8), 8-12.

Chaturvedi, M., Bassin, J., 2010. Assessing the water quality index of water treatment plant and bore wells, in Delhi, India. Environmental monitoring and assessment 163(1), 449-453.

Chen, Z., Yao, L., Yang, J., 2013. Effective availability simulation evaluation research on complex ship system, 2013 International Conference on Quality, Reliability, Risk, Maintenance, and Safety Engineering (QR2MSE). IEEE, pp. 1271-1273.

Chou, F.N.-F., Wu, C.-W., 2015. Stage-wise optimizing operating rules for flood control in a multi-purpose reservoir. Journal of Hydrology 521, 245-260.

Debels, P., Figueroa, R., Urrutia, R., Barra, R., Niell, X., 2005. Evaluation of water quality in the Chillán River (Central Chile) using physicochemical parameters and a modified water quality index. Environmental monitoring and assessment 110(1), 301-322.

Demir, V., Kisi, O., 2016. Flood hazard mapping by using geographic information system and hydraulic model: Mert River, Samsun, Turkey. Advances in Meteorology 2016.

Distefano, S., Puliafito, A., 2007. Dynamic reliability block diagrams vs dynamic fault trees, 2007 Annual Reliability and Maintainability Symposium. IEEE, pp. 71-76.

Distefano, S., Xing, L., 2006. A new approach to modeling the system reliability: dynamic reliability block diagrams, RAMS'06. Annual Reliability and Maintainability Symposium, 2006. IEEE, pp. 189-195.

dos Santos Simões, F., Moreira, A.B., Bisinoti, M.C., Gimenez, S.M.N., Yabe, M.J.S., 2008. Water quality index as a simple indicator of aquaculture effects on aquatic bodies. Ecological indicators 8(5), 476-484.

El Afandi, G., Morsy, M., El Hussieny, F., 2013. Heavy rainfall simulation over sinai peninsula using the weather research and forecasting model. International Journal of Atmospheric Sciences 2013.

Feng, W., Zhou, N., Chen, L., Li, B., 2013. An optical sensor for monitoring of dissolved oxygen based on phase detection. Journal of Optics 15(5), 055502.

Fu, Q., Wang, H., Yan, X., 2019. Evaluation of the aeroengine performance reliability based on generative adversarial networks and Weibull distribution. Proceedings of the Institution of Mechanical Engineers, Part G: Journal of Aerospace Engineering 233(15), 5717-5728.

Georgesce, L., TOPA, M., TIMOFTI, M., BURADA, A., 2015. Danube water quality during and after flood near an urban agglomeration. Journal of Environmental Protection and Ecology 16(4), 1255-1261.

Goel, P., 2006. Water pollution: causes, effects and control. New Age International.

Green, C.H., Parker, D.J., Tunstall, S.M., 2000. Assessment of flood control and management options. WCD Thematic reviews. World Commission on Dams Secretariat, South Africa.

Guo, H., Yang, X., 2007. A simple reliability block diagram method for safety integrity verification. Reliability Engineering & System Safety 92(9), 1267-1273.

Hammond, M.J., Chen, A.S., Djordjević, S., Butler, D., Mark, O., 2015. Urban flood impact assessment: A state-of-the-art review. Urban Water Journal 12(1), 14-29.

Hey, D.L., Philippi, N.S., 1995. Flood reduction through wetland restoration: the Upper Mississippi River Basin as a case history. Restoration Ecology 3(1), 4-17.

Huang, Q., Bando, Y., Zhao, L., Zhi, C., Golberg, D., 2009. pH sensor based on boron nitride nanotubes. Nanotechnology 20(41), 415501.

Huang, W.-D., Cao, H., Deb, S., Chiao, M., Chiao, J.-C., 2011. A flexible pH sensor based on the iridium oxide sensing film. Sensors and Actuators A: Physical 169(1), 1-11.

Hussain, I., Ahamad, K., Nath, P., 2016. Water turbidity sensing using a smartphone. Rsc Advances 6(27), 22374-22382.

Kang, D.-H.D., Kim, J.-G.J., Verma, V., Leon, A.S., Kang, B., 2019. Evaluation of Urban Inundation under Changing Landcover—Application of EPA SWMM-LID to Andong City in South Korea, World Environmental and Water Resources Congress 2019: Hydraulics, Waterways, and Water Distribution Systems Analysis. American Society of Civil Engineers Reston, VA, pp. 83-88.

Kannel, P.R., Lee, S., Lee, Y.-S., Kanel, S.R., Khan, S.P., 2007. Application of water quality indices and dissolved oxygen as indicators for river water classification and urban impact assessment. Environmental monitoring and assessment 132(1), 93-110.

Kececioglu, D., 2003. Maintainability, availability, and operational readiness engineering handbook. DEStech Publications, Inc.

Khan, A.A., Paterson, R., Khan, H., 2003. Modification and application of the CCME WQI for the communication of drinking water quality data in Newfoundland and Labrador, 38th, Central Symposium on Water Quality Research, Canadian Association on Water Quality. pp. 10-11.

Klaassen, K.B., Peppen, J.C.L.V., 1990. A review of: "SYSTEM RELIABILITY:" Concept and Applications. Edward Arnold, New York, 1990. 256 pages. International Journal of General Systems 18(2), 182-182.

Knebl, M., Yang, Z.-L., Hutchison, K., Maidment, D., 2005. Regional scale flood modeling using NEXRAD rainfall, GIS, and HEC-HMS/RAS: a case study for the San Antonio River Basin Summer 2002 storm event. Journal of Environmental Management 75(4), 325-336.

Kunkel, K.E., 2003. North American trends in extreme precipitation. Natural hazards 29(2), 291-305.

Lee, S.-Y., Hamlet, A.F., Fitzgerald, C.J., Burges, S.J., 2009. Optimized flood control in the Columbia River Basin for a global warming scenario. Journal of water resources planning and management 135(6), 440-450.

Leon, A.S., Tang, Y., Chen, D., Yolcu, A., Glennie, C., Pennings, S.C., 2018. Dynamic management of water storage for flood control in a wetland system: a case study in Texas. Water 10(3), 325.

Leon, A.S., Verma, V., 2019. Towards Smart and Green Flood Control: Remote and Optimal Operation of Control Structures in a Network of Storage Systems for Mitigating Floods, World Environmental and Water Resources Congress 2019. pp. 177-189.

Loloee, R., Askeland, P.A., Ghosh, R.N., 2007. Dissolved oxygen sensing in a flow stream using Molybdenum Chloride optical Indicators, SENSORS, 2007 IEEE. IEEE, pp. 1404-1407.

McDonagh, C., Kolle, C., McEvoy, A., Dowling, D., Cafolla, A., Cullen, S., MacCraith, B., 2001. Phase fluorometric dissolved oxygen sensor. Sensors and Actuators B: Chemical 74(1-3), 124-130.

Mel, R.A., Viero, D.P., Carniello, L., D'Alpaos, L., 2020. Optimal floodgate operation for river flood management: The case study of Padova (Italy). Journal of Hydrology: Regional Studies 30, 100702.

Ming, J., Xian-Guo, L., Lin-Shu, X., Li-juan, C., Shouzheng, T., 2007. Flood mitigation benefit of wetland soil—A case study in Momoge National Nature Reserve in China. Ecological Economics 61(2-3), 217-223.

Mitsch, W.J., Bernal, B., Hernandez, M.E., 2015. Ecosystem services of wetlands. Taylor & Francis.

Ott, W.R., 1978. water quality indices: a survey of indices used in the United States. Environmental Protection Agency, Office of Research and Development, Office ….

Ozecik, D., 2021. An integrated software and hardware architecture for gravity driven and remotely operated water release (master's thesis). Florida International University, Miami, Florida.

Parra, L., Rocher, J., Escrivá, J., Lloret, J., 2018. Design and development of low cost smart turbidity sensor for water quality monitoring in fish farms. Aquacultural Engineering 81, 10-18.

Praveen, P.K., Ganguly, S., Kumar, K., Kumari, K., 2016. Water pollution and its hazardous effects to human health: A review on safety measures for adoption. Int J. Sci Technol. 2016a 5, 1559-1563.

Qin, L., Leon, A.S., Bian, L., Dong, L., Verma, V., Yolcu, A., 2019. A Remotely-Operated Siphon System for Water Release From Wetlands and Shallow Ponds. IEEE Access 7, 157680-157687.

Rausand, M., Høyland, A., 2003. System reliability theory: models, statistical methods, and applications. John Wiley & Sons.

Rossiter, H.M.A., Owusu, P.A., Awuah, E., MacDonald, A.M., Schäfer, A.I., 2010. Chemical drinking water quality in Ghana: Water costs and scope for advanced treatment. Science of The Total Environment 408(11), 2378-2386.

Saeedi, M., Abessi, O., Sharifi, F., Meraji, H., 2010. Development of groundwater quality index. Environmental monitoring and assessment 163(1), 327-335.

Sánchez, E., Colmenarejo, M.F., Vicente, J., Rubio, A., García, M.G., Travieso, L., Borja, R., 2007. Use of the water quality index and dissolved oxygen deficit as simple indicators of watersheds pollution. Ecological indicators 7(2), 315-328.

Scholz, M., 2011. Introduction to Wetland Systems, Wetland Systems. Springer, pp. 1-17.

Seidel, M.P., DeGrandpre, M.D., Dickson, A.G., 2008. A sensor for in situ indicator-based measurements of seawater pH. Marine chemistry 109(1-2), 18-28.

Sene, K., 2008. Flood warning, forecasting and emergency response. Springer Science & Business Media.

Shamsai, A., Urei, S., Sarang, A., 2006. Comparative of qualitative indexes and qualitative zoning of Karoon river and Dez river. Journal of Water and Wastewater 16, 88-97.

Shao, W., Li, Y., Yan, D., Liu, J., Yang, Z., Yang, Z., 2018. Analysis of the Losses Due to Flood and Waterlogging Disasters in China during 2006 to 2017, Multidisciplinary Digital Publishing Institute Proceedings. p. 25.

Shenoy, M.R., Pal, B.P., Gupta, B.D., 2011. Design, analysis, and realization of a turbidity sensor based on collection of scattered light by a fiber-optic probe. IEEE Sensors Journal 12(1), 44-50.

Shimi, A.C., 2010. Gulsan Ara Parvin, Chaitee Biswas, and Rajib Shaw. 2010."Impact and Adaptation to Flood: A Focus on Water Supply, Sanitation and Health Problems of Rural Community in Bangladesh.". Disaster Prevention and Management 19(3), 298-313.

Simić, M., Manjakkal, L., Zaraska, K., Stojanović, G.M., Dahiya, R., 2016. TiO 2-based thick film pH sensor. IEEE Sensors Journal 17(2), 248-255.

Son, C.-H., Baek, J.-I., Ban, Y.-U., Ha, S.-R., 2015. The effects of mitigation measures on flood damage prevention in Korea. Sustainability 7(12), 16866-16884.

Subyani, D., Daniels, A., Murray, S., Kirsch, T., 2017. The human impact of floods: a historical review of events 1980–2009 and systematic literature review. PLoS Curr 5, 1-19.

Thampapillai, D.J., Musgrave, W.F., 1985. Flood damage mitigation: A review of structural and nonstructural measures and alternative decision frameworks. Water Resources Research 21(4), 411-424.

Tian, X., 2006. Cooling fan reliability: failure criteria, accelerated life testing, modeling and qualification, RAMS'06. Annual Reliability and Maintainability Symposium, 2006. IEEE, pp. 380-384.

Tsegaye, T., Sheppard, D., Islam, K., Tadesse, W., Atalay, A., Marzen, L., 2006. Development of chemical index as a measure of in-stream water quality in response to land-use and land cover changes. Water, Air, and Soil Pollution 174(1), 161-179.

Verma, V., Bian, L., Rojali, A., Ozecik, D., Leon, A., 2020a. A Remotely Controlled Framework for Gravity-Driven Water Release in Shallow and Not Shallow Storage Ponds, World Environmental and Water Resources Congress 2020. pp. 12-22.

Verma, V., Vutukuru, K.S., Bian, L., Rojali, A., Ozecik, D., Leon, A., 2020b. Reliability and Robustness Evaluation of a Remotely Operated Siphon System for Flood Mitigation during Hurricanes, World Environmental and Water Resources Congress 2020. pp. 31-39.

Wang, W., Loman, J.M., Arno, R.G., Vassiliou, P., Furlong, E.R., Ogden, D., 2004. Reliability block diagram simulation techniques applied to the IEEE std. 493 standard network. IEEE Transactions on Industry Applications 40(3), 887-895.

Yang, S.-I., Frangopol, D.M., Neves, L.C., 2006. Optimum maintenance strategy for deteriorating bridge structures based on lifetime functions. Engineering structures 28(2), 196-206.

Yigzaw, W., Hossain, F., Kalyanapu, A., 2013. Impact of artificial reservoir size and land use/land cover patterns on probable maximum precipitation and flood: Case of Folsom Dam on the American River. Journal of Hydrologic Engineering 18(9), 1180-1190.

Zhang, T., Xie, M., 2007. Failure data analysis with extended Weibull distribution. Communications in Statistics—Simulation and Computation® 36(3), 579-592.

VITA

VIVEK VERMA
Born, Durg, Chhattisgarh, India

2011-2015	B.E., Civil Engineering, SSIPMT, Raipur, India
2015-2017	M.S., Civil Engineering, Texas A&M University, Texas
	Research Assistant Texas A&M University, Texas
2020-2021	Doctoral Candidate Florida International University, Florida
	Teaching Assistant Florida International University, Florida
	Research Assistant Florida International University, Florida

PUBLICATIONS AND PRESENTATIONS

Verma, V., Bian, L., Rojali, A., Ozecik, D., Leon, A., 2020a. A Remotely Controlled Framework for Gravity-Driven Water Release in Shallow and Not Shallow Storage Ponds, World Environmental and Water Resources Congress 2020. pp. 12-22.

Verma, V., Vutukuru, K.S., Bian, L., Rojali, A., Ozecik, D., Leon, A., 2020b. Reliability and Robustness Evaluation of a Remotely Operated Siphon System for Flood Mitigation during Hurricanes, World Environmental and Water Resources Congress 2020. pp. 31-39.

Leon, A.S., Verma, V., 2019. Towards Smart and Green Flood Control: Remote and Optimal Operation of Control Structures in a Network of Storage Systems for Mitigating Floods, World Environmental and Water Resources Congress 2019. pp. 177-189.

Qin, L., Leon, A.S., Bian, L., Dong, L., Verma, V., Yolcu, A., 2019. A Remotely-Operated Siphon System for Water Release From Wetlands and Shallow Ponds. IEEE Access 7, 157680-157687.